Chapter 11

GRAIN GROWTH FOLLOWING RECRYSTALLIZATION

11.1 INTRODUCTION

Compared with primary recrystallization, the growth of grains in a recrystallized single-phase material might appear to be a relatively simple process. However, despite a large amount of theoretical and experimental effort, many important questions remain unanswered. The theoretical basis for understanding grain growth was laid down over 50 years ago in the classic papers of Smith (1948, 1952) and Burke and Turnbull (1952), and the apparent conflict of theory with experiment prompted several other theoretical models over a period of some 30 years. The application of computer simulation techniques (Anderson et al. 1984) provided a fresh approach to the problem and the interest and controversy surrounding the computer simulations gave a stimulus to the subject, which resulted in a number of international conferences (§1.2.2) and a large volume of literature.

Although primary recrystallization often precedes grain growth, it is of course not a necessary precursor, and the contents of this chapter are equally relevant to grain growth in materials produced by other routes, such as casting or vapour deposition. In this chapter we consider only the growth of grains under the driving pressures due to boundaries in the material. However, we note here that boundaries can be induced to

migrate by externally applied forces such as those due to stress as discussed in §5.2.1 or by magnetic fields (e.g. Smolukowski and Turner 1949, Watanabe 2001).

In this chapter we are primarily concerned with the **kinetics of grain growth** and the nature and **stability of the microstructure**; the factors affecting the **mobilities of the grain boundaries** are discussed in chapter 5.

11.1.1 The nature and significance of grain growth

When primary recrystallization, which is driven by the stored energy of cold work, is complete, the structure is not yet stable, and further growth of the recrystallized grains may occur. The driving force for this is a reduction in the energy which is stored in the material in the form of grain boundaries. The driving pressure for grain growth is often some two orders of magnitude less than that for primary recrystallization (§1.3.2), and is typically $\sim 10^{-2}$ MPa. Consequently, at a particular temperature, grain boundary velocities will be slower than during primary recrystallization, and boundary migration will be much more affected by the pinning effects of solutes and second-phase particles.

The technological importance of grain growth stems from the dependence of properties, and in particular the mechanical behaviour, on grain size. In materials for structural application at lower temperatures, a small grain size is normally required to optimise the strength and toughness. However, in order to improve the high temperature creep resistance of a material, a large grain size is required. Examples of the application of the control of grain growth which are considered in chapter 15, include the processing of silicon–iron transformer sheet and the development of microstructures for superplastic materials. There is also considerable interest in grain growth in thin metal, oxide and semiconductor films for electronic applications as discussed in §11.5.4. A good understanding of grain growth is therefore a pre-requisite for control of the microstructures and properties of metals and ceramics during solid state processing.

Grain growth may be divided into two types, **normal grain growth** and **abnormal grain growth or secondary recrystallization.** Normal grain growth, in which the microstructure coarsens uniformly, is classified as a **continuous process.** There is a relatively narrow range of grain sizes and shapes, and the form of the grain size distribution is usually independent of time and hence of scale as shown in figure 11.1a. After an initial transient period of growth, the microstructure reaches a **quasi-stationary state** in which the grain size distribution has an invariant form when expressed in terms of the grain size scaled by its mean value, and only the scale varies with some power of time. Such **self-similarity** is found for several growth processes such as particle coarsening or bubble growth (Mullins 1986), making this a challenging problem for modellers, who are often attracted more by the mathematical intricacies than the intrinsic importance of grain growth.

During abnormal grain growth, which is a **discontinuous** process, a few grains in the microstructure grow and consume the matrix of smaller grains and a bimodal grain size distribution develops. However, eventually these large grains impinge and normal grain growth may then resume (fig. 11.1b).

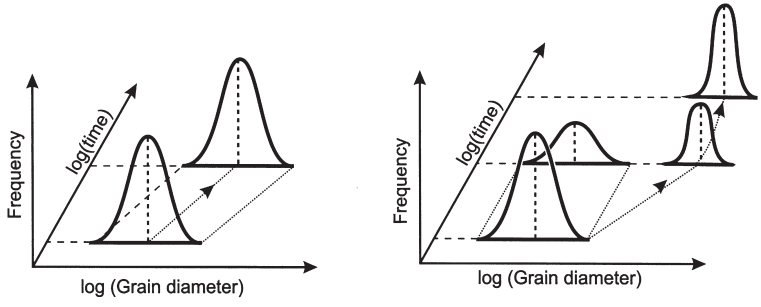

(a) (b)

Fig. 11.1. Schematic representation of the change in grain size distribution during (a) Normal grain growth and (b) Abnormal grain growth, (After Detert 1978).

11.1.2 Factors affecting grain growth

The main factors which influence grain growth, and which will be considered later in this chapter include:

- **Temperature**

Grain growth involves the migration of high angle grain boundaries and the kinetics will therefore be strongly influenced by the temperature dependence of boundary mobility as discussed in §5.3.1. Because the driving force for grain growth is usually very small, significant grain growth is often found only at very high temperatures.

- **Solutes and particles**

Although grain growth is inhibited by a number of factors, the pinning of grain boundaries by solutes (§5.3.3) and by second-phase particles (§4.6) is particularly important.

- **Specimen size**

The rate of grain growth diminishes when the grain size becomes greater than the thickness of a sheet specimen. In this situation the columnar grains are curved only in one direction rather than two, and thus the driving force is diminished. The grain boundaries, where they intersect the surface, may also develop grooves by thermal etching, and these will impede further grain growth.

- **Texture**

A strongly textured material inevitably contains many low angle boundaries of low energy, and there is therefore a reduced driving force for grain growth.

11.1.3 The Burke and Turnbull analysis of grain growth kinetics

Burke (1949) and Burke and Turnbull (1952) deduced the kinetics of grain growth on the assumption that the driving pressure (**P**) on a boundary arises only from the

curvature of the boundary. If the principal radii of curvature of a boundary of energy γ_b are $\mathbf{R_1}$ and $\mathbf{R_2}$ then

$$P = \gamma_b\left(\frac{1}{R_1}+\frac{1}{R_2}\right) \tag{11.1}$$

If the boundary is part of a sphere of radius $\mathbf{R}$, then $\mathbf{R = R_1 = R_2}$ and

$$P = \frac{2\gamma_b}{R} \tag{11.2}$$

Burke and Turnbull then made the following assumptions:

- **γ_b is the same for all boundaries.**
- **The radius of curvature (R) is proportional to the mean radius ($\bar{R}$) of an individual grain, and thus**

$$P = \frac{\alpha\gamma_b}{\overline{R}} \tag{11.3}$$

where α is a small geometric constant.

- **The boundary velocity is proportional to the driving pressure P** (equation 5.1), and to **dR/dt**. i.e. **dR/dt = cP**, where c is a constant.

Hence,

$$\frac{d\overline{R}}{dt} = \frac{\alpha c_1 \gamma_b}{\overline{R}} \tag{11.4}$$

and therefore

$$\overline{R}^2 - \overline{R}_0^2 = 2\alpha c_1 \gamma_b t$$

which may be written as

$$\overline{R}^2 - \overline{R}_0^2 = c_2 t \tag{11.5}$$

where $\bar{\mathbf{R}}$ is the mean grain size at time **t**, $\overline{R}_0$ is the initial mean grain size and $\mathbf{c_2}$ is a constant.

This **parabolic growth law** is expected to be valid for both 2-D and 3-D microstructures, although, according to equation 11.1 the constant c_2 will be different for the two situations. In the limit where $\overline{R}^2 \gg \overline{R}_0^2$

$$\overline{R}^2 = c_2 t \tag{11.6}$$

Equations 11.5 and 11.6 may be written in the more general form

$$\overline{R}^n - \overline{R}_0^n = c_2 t \tag{11.7}$$

$$\overline{R} = c_2 t^{1/n} \tag{11.8}$$

The constant **n**, often termed the **grain growth exponent** is, in this analysis equal to **2**.

11.1.4 Comparison with experimentally measured kinetics

The use of equations 11.5 and 11.6 to describe grain growth kinetics was first suggested empirically by Beck et al. (1949). These authors found that **n** was generally well above 2 and that it varied with composition and temperature. It is significant that very few measurements of grain growth kinetics have produced the grain growth exponent of 2 predicted by equations 11.5 or 11.6, and values of **1/n** for a variety of metals and alloys as a function of homologous temperature are shown in figure 11.2. The trend towards lower values of **n** at higher temperatures, seen in this figure, has been reported in many experiments.

Data for some zone-refined metals in which the impurity levels are no more than a few ppm are shown in table 11.1. The values of **n** range from 2 to 4, with an average of 2.4 ± 0.4. Grain growth kinetics have been extensively measured in ceramics, and compilations of the data (Anderson et al. 1984, Ralph et al. 1992) reveal a similar range of grain growth exponents as is shown in table 11.2.

Much effort has been expended in trying to explain why the measured grain growth exponents differ from the 'theoretical' value of 2 given by the Burke and Turnbull analysis, and the earlier explanations fall into two categories:

(i) The boundary mobility (M) varies with the boundary velocity
The boundary mobility, as discussed in §5.1.3, may under certain circumstances be a function of boundary velocity, in which case the linear dependence of velocity on driving pressure (equation 5.1), which is assumed in the Burke and Turnbull analysis will not apply. An example of this is the case of solute drag on boundaries (§5.4.2). Figure 5.32 shows that the velocity is not linearly proportional to the driving pressure except for very low or very high boundary velocities. However, the shape of these curves

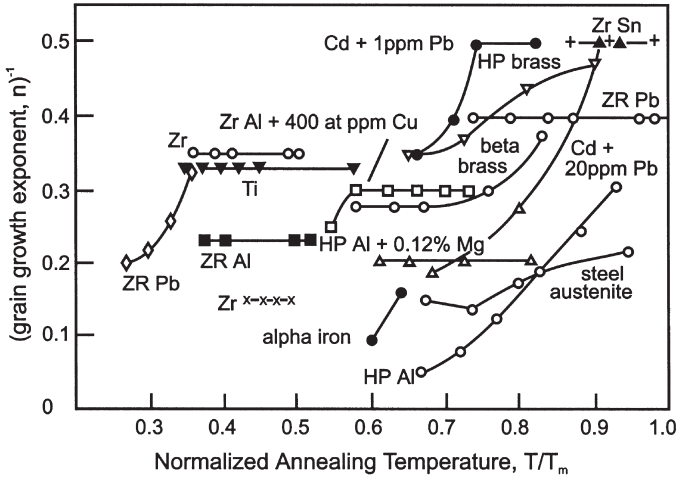

Fig. 11.2. The temperature dependence of the grain growth exponent **n** for isothermal grain growth in a variety of materials, (Higgins 1974).

Table 11.1
Grain growth exponents for isothermal grain growth in high purity metals (from Anderson et al. 1984).

Metal	Exponent n	Reference
Al	4	Gordon and El Bassyoumi (1965)
Fe	2.5 (varies with T)	Hu (1974)
Pb	2.5	Bolling and Winegard (1958)
Pb	2.4	Drolet and Gallibois (1968)
Sn	2.3	Drolet and Gallibois (1968)

Table 11.2
Grain growth exponents for isothermal grain growth in ceramics (from Anderson et al. 1984).

Ceramic	Exponent n	Reference
ZnO	3	Dutta and Spriggs (1970)
MgO	2	Kapadia and Leipold (1974)
MgO	3	Gordon et al. (1970)
CdO	3	Petrovic and Ristic (1980)
$Ca_{0.16}Zr_{0.84}O_{1.84}$	2.5	Tien and Subbaro (1963)

would only predict a higher grain growth exponent if conditions were such that the boundary changed from breakaway to solute drag behaviour during grain growth, and it is unlikely that these conditions would commonly be met.

As discussed in §5.3.1.2, there is evidence of changes in grain boundary structure and mobility at very high temperatures, even in metals of very high purity. It is conceivable that this could account in some cases for transitions to lower **n** values, although there is no direct evidence for this.

Grain growth in ceramics has been extensively investigated, and in many cases the measured values of **n** have been ascribed to particular mechanisms of boundary migration. For example Brook (1976) lists eleven proposed mechanisms for boundary migration with growth exponents of between 1 and 4.

(ii) There is a limiting grain size
An alternative empirical analysis of the data was given by Grey and Higgins (1973), who proposed that equation 5.1 be replaced by

$$v = M(P - C) \tag{11.9}$$

where **C** is a constant for the material.

If this relationship is used in the Burke and Turnbull analysis then equation 11.4 becomes

$$\frac{d\overline{R}}{dt} = c_1\left(\frac{\alpha\gamma_b}{\overline{R}} - C\right) \tag{11.10}$$

When, as a result of grain growth, the driving pressure **P** falls to the value **C**, there is no net pressure, and grain growth ceases at a **limiting value.** Grey and Higgins showed that this form of equation accounted quite well for the kinetics of grain growth in several materials. The term **C** is similar to the Zener pinning term which accounts for a limiting grain size in two-phase materials (§11.4.2), and Grey and Higgins suggested that the physical origin of **C** might be solute clusters which are unable to diffuse with the boundary.

However, there is often little evidence for $\mathbf{n = 2}$ even in very pure materials, and it has been suggested that one or more of the underlying assumptions of the Burke and Turnbull analysis may be incorrect. Although we will later conclude that there is little evidence to suggest that the Burke and Turnbull result is in serious error, a great deal of work has gone into producing more refined models of grain growth which address not only the kinetics but also the grain size distribution.

11.1.5 Topological aspects of grain growth

The Burke and Turnbull analysis assumes that the mean behaviour of the whole array of grains can be inferred from the migration rate of part of one boundary and does not consider the interaction between grains or the constraints imposed by the space-filling requirements of the microstructure. This aspect of grain growth was first addressed by Smith (1952) who discussed grain growth in terms of grain topology and stated that **'Normal grain growth results from the interaction between the topological requirements of space-filling and the geometrical needs of surface tension equilibrium'.**

From the introduction to grain topology in §4.5, we note that in a two-dimensional grain structure, the only stable arrangement which can fulfil both the space-filling and boundary tension equilibrium requirements is an array of regular hexagons as shown in figure 11.3, and any other arrangement must inevitably lead to grain growth. For example, if just one 5-sided polygon is introduced (fig. 11.4a), then it must be balanced by a 7-sided one to maintain the average number of edges per grain at 6 (§4.5.1) as shown in figure 11.4a. In order to maintain the 120° angles at the vertices, the sides of the grains must become curved. Grain boundary migration then tends to occur in order to reduce the boundary area, and the boundaries migrate towards their centres of curvature (fig. 11.4b). Any grain with more than six sides will tend to grow because its boundaries are concave and any grain with less than six sides will tend to shrink as it has convex sides. The shrinkage of the 5-sided grain in figure 11.4a leads to the formation of a 4-rayed vertex (fig. 11.4b) which decomposes into two 3-rayed vertices and the grain becomes 4-sided (fig. 11.4c). A similar interaction allows the grain to become 3-sided (fig. 11.4e) and to eventually disappear leaving a 5-sided grain adjoining a 7-sided grain (fig. 11.4f).

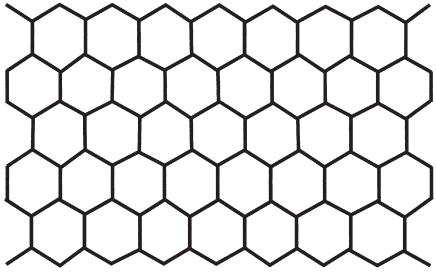

Fig. 11.3. A 2-dimensional array of equiaxed hexagonal grains is stable.

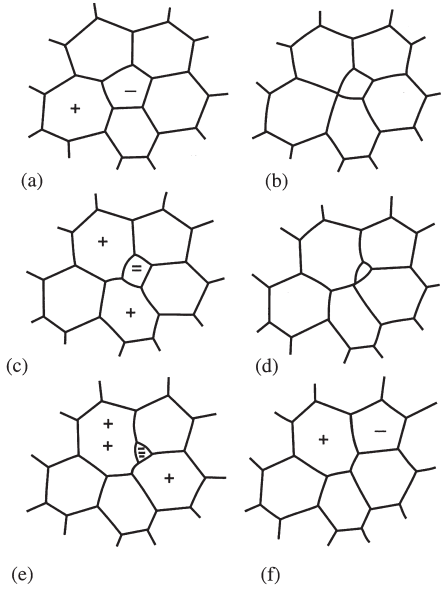

Fig. 11.4. Schematic diagram of growth of a 2-dimensional grain structure. (a) A grain of less than or more than 6 sides introduces instability into the structure, (b)–(f) Shrinking and disappearance of the 5-sided grain, (Hillert 1965).

Von Neumann (1952) and Mullins (1956) proposed on the basis of surface tension requirements, that the growth of a 2-D cell of area **A** with **N** sides is given by

$$\frac{dA}{dt} = c(N - 6) \tag{11.11}$$

or, if written in terms of grain radius (R)

$$\frac{dR}{dt} = \frac{c(N - 6)}{2R} \tag{11.12}$$

Rivier (1983) later showed that the **Von Neumann–Mullins law** is actually a geometric result and not due to surface tension.

In three dimensions, no regular polyhedron with plane sides can fill space and have its sides at the appropriate angles to balance the boundary tensions. As discussed in §4.5, the nearest shape is the Kelvin tetrakaidecahedron (fig. 4.17) but the angles are not exact and the boundaries must become curved to obtain equilibrium at the vertices. Therefore **grain growth is inevitable in an ideal 3-dimensional grain structure.**

11.2 THE DEVELOPMENT OF THEORIES AND MODELS OF GRAIN GROWTH

A complete theory of grain growth must take into account both the topological space-filling requirements discussed by Smith and the kinetics of local boundary migration as discussed by Burke and Turnbull. In this section we review the various attempts that have been made to improve on the theory discussed in §11.1.3. We should note that all the theories discussed below assume that the rate limiting factor in grain growth is the migration of the boundaries. However, grain growth also involves the migration of grain vertices, and the possibility that the mobility of these defects might become rate limiting under certain circumstances as discussed in §5.5, should not be ignored, although it appears likely that this is only significant for nano-structured materials.

11.2.1 Introduction

Because the geometry of an array of grains is very similar to that of a soap froth, and the stability and evolution of the latter is of interest in its own right, this analogy has been widely studied. For example Smith (1952) suggested, on the basis of data from soap froth experiments that the distribution of grain sizes and shapes should be invariant, and that the grain area should be proportional to time. In both systems the driving force for growth is the reduction in boundary energy. The analogy between the two cases is very close, and similar growth kinetics and grain size distributions are found, as discussed by Weaire and Rivier 1984, Atkinson 1988 and Weaire and Glazier 1992. However, the mechanisms of growth are different because in froths, growth occurs by gas molecules permeating through the cell membranes in order to equalise the pressures. There are other significant differences, and there are therefore limits to the extent that soap froth evolution can be used as an analogy for grain growth.

Theories and models of grain growth may be divided into two general categories, **deterministic** and **statistical**. Deterministic models are based on the premise that the behaviour of any grain in the assembly is dependent upon the behaviour of **all** the other grains. If the geometry of the whole grain assembly is known, then topological constraints are automatically accounted for, and by the application of relatively simple local rules such as equation 11.4, the evolution of the grain structure is predicted. This very powerful approach requires extensive computing power if reasonable sized grain assemblies are to be studied, and deterministic models will be further discussed in §11.2.4.

Statistical models are based on the assumption that the behaviour of the whole grain assembly can be calculated by generalising the behaviour of a small part of the microstructure. The Burke and Turnbull analysis is an example of such a model, and the later refinements which predict grain size distributions and which approximate the topographical constraints are discussed in §11.2.2 and §11.2.3.

The development of statistical theories of grain growth has a long and complex history and the merits of different approaches are still hotly debated. The essential problem is that the theories need to reduce the topological complexity of the real grain structure and its effect on the driving forces for grain growth to some average value, with a manageable number of parameters, for the particular grain under consideration. In assessing the theories we will concentrate on their predictions of the kinetics of grain growth and of the grain size distributions, and the comparison of these experimentally.

11.2.2 Early statistical theories

The majority of statistical grain growth theories fall into the category of **mean field theories** which determine the behaviour of a single grain or boundary in an environment which is some average representation of the whole assembly. The theories may be divided into two groups. During grain growth, the larger grains grow and the smaller grains shrink and statistically the grains can be considered to move in grain size–time–space under the action of a force which causes a drift in the mean grain size. Such models, typified by the theories of Feltham and Hillert are commonly known as **drift models.** Another approach, taken by Louat, is to consider the grain faces to undergo a random walk in the grain size–time–space. Grain growth then formally becomes a diffusion-like process, and this is often known as the **diffusion model.**

11.2.2.1 Feltham and Hillert's theories

Hillert (1965) developed a statistical theory of grain growth which was based on the assumption that the grain boundary velocity is inversely proportional to its radius of curvature. He used previous analyses of the Ostwald ripening of a distribution of second-phase particles to obtain the relationship

$$\frac{dR}{dt} = cM\gamma_b\left(\frac{1}{R_{crit}} - \frac{1}{R}\right) \tag{11.13}$$

where $c = 0.5$ for a 2-D array and 1 for a 3-D array. R_{crit} is a critical grain size which varies with time according to

$$\frac{d(R_{crit}^2)}{dt} = \frac{cM\gamma_b}{2} \tag{11.14a}$$

$$\frac{dR_{crit}}{dt} = \frac{cM\gamma_b}{4R_{crit}} \tag{11.14b}$$

A grain such that $R < R_{crit}$ will shrink, and one with $R > R_{crit}$ will grow. Hillert showed that topographic considerations resulted in the mean grain radius $\bar{R}$ being equal to R_{crit},

and therefore equation 11.14 predicts parabolic grain growth kinetics of the form of equations 11.4 and 11.5.

Hillert also solved equation 11.13 to obtain the grain size distribution f(R,t). As shown in figure 11.6a, this is much narrower than the log-normal distribution which is close to that found experimentally (§11.2.4 and fig. 11.6b). In Hillert's grain size distribution the maximum was $1.8\bar{R}$ for a 3-D array and $1.7\bar{R}$ for a 2-D array. He argued that if the initial grain size distribution contained no grains larger than $1.8\bar{R}$ then normal grain growth would result and the distribution would adjust to the predicted f(R,t). However, if grains larger than $1.8\bar{R}$ were present then he predicted that abnormal grain growth would result, although this latter conclusion has been shown to be incorrect (§11.5.1).

Hillert's result is very similar to that obtained by Feltham (1957), who started from the assertion that the normalised grain size distribution was log-normal and time invariant. He obtained

$$\frac{dR^2}{dt} = c \ln\left(\frac{R}{\bar{R}}\right) \tag{11.15}$$

where c is a constant. Setting $R = R_{max} = 2.5\bar{R}$ he obtained parabolic growth kinetics.

11.2.2.2 Louat's random walk theory

Louat (1974) argued that boundary motion can be analysed as a diffusional process in which sections of the boundary undergo random motion. This will lead to grain growth because the process of grain loss by shrinkage is not reversible. The theory predicts parabolic grain growth kinetics and an invariant Rayleigh grain size distribution (fig. 11.6a) which is close to that found experimentally (§11.2.4). Although the theory has been criticised by a number of authors on the grounds that it lacks a strong physical basis for its assumptions, it was later defended and further developed by its author (Louat et al. 1992). Pande (1987) has developed a statistical model which combines the random walk element of Louat's theory with the radius of curvature approach of Hillert.

11.2.3 The incorporation of topology

11.2.3.1 Defect models

Hillert (1965) proposed an alternative approach to two-dimensional grain growth based on the topological considerations discussed in §11.1.5. Within an array of six-sided grains, the introduction a 5-sided and 7-sided grain as shown in figure 11.4a, constitutes a stable defect. As growth occurs and the 5-sided grain ultimately disappears (fig. 11.4b–e), the 5–7 pair defect moves through the structure (fig. 11.4f). Hillert argued that the rate of growth depended on the time taken for the defect to move (i.e. for a 5-sided grain to shrink) and on the number of such defects in the microstructure. If the latter remained constant, which is a reasonable assumption for a time invariant grain distribution, then a parabolic growth rate similar to that for his statistical theory (equation 11.14) results. Morral and Ashby (1974) extended this model to 3-D by introducing 13 or 15-sided grains into an array of 14-sided polyhedra.

11.2.3.2 The Rhines and Craig analysis

Rhines and Craig (1974) emphasised the role of topology in grain growth. They argued that when a grain shrinks and disappears as shown in figure 11.4, then not only must this volume be shared out between the neighbouring grains, but because the topological attributes (shape, faces, edges, vertices etc.) of the neighbours also alter, this will in turn influence grains which are further away. They introduced two new concepts, the **sweep constant** and the **structural gradient.**

They defined a **sweep constant** Θ, as the number of grains lost when the grain boundaries in the specimen sweep out unit volume of material. They argued that Θ will remain constant during grain growth. An alternative parameter Θ^*, the number of grains lost when the boundaries sweep through a volume of material equal to that of the mean grain volume, was suggested by Doherty (1975). Clearly both these parameters cannot remain constant during grain growth, neither can be measured directly by experiment, and the matter is unresolved. The second parameter introduced by Rhines and Craig was the dimensionless **structural gradient** ς, which is the product of the **surface area per unit volume (S_v)** and the **surface curvature per grain (m_v/N_v)**. i.e.

$$\varsigma = \frac{m_v S_v}{N_v} \tag{11.16}$$

where N_v is the number of grains per unit volume and

$$m_V = \int_{S_V} \frac{1}{2}\left(\frac{1}{r_1} + \frac{1}{r_2}\right) dS_V \tag{11.17}$$

where r_1 and r_2 are the principal radii of curvature.

Rhines and Craig argued that ς should remain constant during growth and as shown in figure 11.5a, found ς to be constant in their experiments. However, Doherty (1975) suggested an alternative structure gradient $\varsigma^* = m_v/N_v$, which is the mean curvature per grain.

The Rhines and Craig analysis, using Doherty's modifications as suggested by Atkinson (1988) is as follows. The mean pressure (P) on the boundaries is

$$P = \frac{\gamma_b m_v}{S_v} \tag{11.18}$$

and the mean boundary velocity

$$v = MP = \frac{M\gamma_b m_V}{S_V} \tag{11.19}$$

The volume swept per second per unit volume of specimen is $v.S_v$, and if Θ^* grains are lost per unit volume, for each $\bar{V}$ (where $N_v = \bar{V}^{-1}$), the rate of loss of grains will be

$$\frac{dN_v}{dt} = \frac{\theta^* v S_v}{\bar{V}} = \theta^* M \gamma_b m_v N_v \tag{11.20}$$

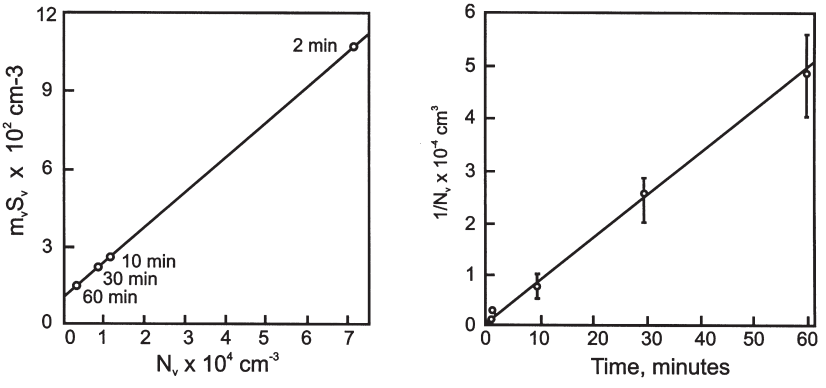

Fig. 11.5. (a) Plot of $m_v S_v$ against N_v for grain growth in aluminium, (b) Plot of mean grain volume ($1/N_v$) against annealing time for aluminium, (after Rhines and Craig 1974).

For each grain lost, per unit volume, there is a net increase in volume of $\bar{V}$ which on average is distributed over the remaining N_v grains. Therefore

$$\frac{d\bar{V}}{dt} = \frac{dN_V}{dt}\frac{\bar{V}}{N_V} = \frac{\theta^* M \gamma_b m_V}{N_V} \tag{11.21}$$

If Θ^*, M, γ_b, and m_v/N_v ($= \varsigma^*$) are constant with time then equation 11.21 can be integrated to give

$$\bar{V} = \frac{\theta^* M \gamma_b m_V t}{N_V} + \bar{V}_0 = ct + \bar{V}_0 \tag{11.22}$$

where $\bar{V}_0$ is the mean grain volume at $t = 0$.

As shown in figure 11.5b, Rhines and Craig (1974) found such a relationship in aluminium of 99.99% purity. A linear dependence of $\bar{V}$ on time implies that the grain radius is growing as $t^{1/3}$, i.e. **the grain growth exponent n of equation 11.7 is equal to 3.** As emphasised by Rhines and Craig (1974), this is an important difference from the value of **2** predicted by most other theories. The linear dependence of $\bar{V}$ on time is only predicted in the above analysis if ς^* remains constant, whereas the results shown in figure 11.5b shown a constancy of ς. Doherty (1975) has suggested that this could be reconciled if in equation 11.18, the driving pressure **P** was replaced by **(P−c)**, in accord with equation 11.9.

The Rhines and Craig experiments were carried out by the very time-consuming method of serial sectioning of specimens rather than by analysis of 2-D sections as is commonly done. They found that conventional 2-D analysis of their specimens resulted in the grain radius being proportional to $t^{0.43}$, i.e. $\mathbf{n = 2.3}$, which is rather close to that commonly

found (table 11.1). They concluded from the discrepancy between their 2-D and 3-D measurements that $\mathbf{N_v}$ **can only be determined from 3-D methods such as serial sectioning and cannot be inferred from measurements on a 2-D section.** There has been widespread discussion of this point, and the analysis of 3-D microstructures produced by computer simulation (Anderson et al. 1984, Srolovitz et al. 1984a) has been of help. These have shown that there will only be a serious discrepancy between 2-D and 3-D metallographic methods if the structure is **anisotropic**, and the difference in the grain growth exponents measured by Rhines and Craig (1974) in 2-D and 3-D therefore implies that their microstructure was anisotropic. There is of course a serious implication in this for all experiments based on 2-D sections, and the work of Rhines and Craig emphasises that grain shape anisotropy must be determined if 2-D measurements are to be used for comparison with theory.

This seminal work left a number of unanswered questions about theoretical and experimental aspects of grain growth kinetics. In particular, it was not clear whether a grain growth exponent of 3 would be the result of any model based on topographic considerations or whether it is specific to this particular analysis. As discussed by Atkinson (1988), it is not obvious that the microstructure will be in topographic equilibrium, particularly at low temperatures, and if this is the case then the local topographic constraints discussed in §11.2.3.1 may be more appropriate. Kurtz and Carpay (1980) proposed a detailed statistical theory of grain growth, which placed an emphasis on topographic considerations, and was essentially an extension of the Rhines and Craig model. However, unlike Rhines and Craig, Kurtz and Carpay predicted a parabolic ($\mathbf{n = 2}$) grain growth relationship.

Because of the difficulty of serial sectioning methods, experimental confirmation of $\bar{V} \propto t$ is limited to the work of Rhines and Craig (1974), and as shown by the results in tables 11.1 and 11.2, it would be inadvisable to place too much reliance on a study of a single material, in particular aluminium of only moderate purity, in which boundary mobility is known to be very sensitive to small amounts of impurity (§5.3.3). However a grain growth exponent of ~3 would not be inconsistent with many investigations of metals.

11.2.3.3 The Abbruzzese–Heckelmann–Lücke model

These authors developed a 2-D statistical theory of grain growth (Lücke et al. 1990, 1992, Abbruzzese et al. 1992). A key element of their approach is the introduction of topological parameters relating the number of sides of a grain ($\bar{n}_i$) to its size (r_i). From experimental measurements they found that

$$\bar{n}_i = 3 + 3r_i \tag{11.23}$$

and that the mean size ($\bar{r}_n$) of grains with **n** sides was given by

$$n = 6 + \frac{3(\bar{r}_n - 1)}{\xi^2} \tag{11.24}$$

where ξ is a correlation coefficient equal to 0.85.

Although this **special linear relationship** is derived from experiments, the authors suggested that it would be generally applicable to equiaxed real grain structures. The parabolic grain growth kinetics predicted on this model are similar to those of the Hillert theory i.e. equation 11.14.

11.2.3.4 Other recent statistical theories

The discussions above show that although statistical theories of normal grain growth in pure single-phase polycrystals have been developed over a period of some 50 years, there is no general agreement as to the correct solution, or even if this type of approach can ever yield a satisfactory solution. New theories and modifications of the old theories are still being produced at an alarming rate as may be seen from the literature and the proceedings of recent conferences on grain growth. One of the main problems in reaching an agreement remains the representation of the topology of the grain structure both accurately and with a reasonable number of parameters.

11.2.4 Deterministic theories

If instead of considering the behaviour of an 'average' grain, we consider the growth and shrinkage of **every grain in the assembly** then many of the topological difficulties of the statistical models are bypassed. Hunderi and Ryum (1992b) discuss the relative merits of **statistical** and **deterministic** models of grain growth and illustrate this with an analysis of grain growth in one dimension, developed from the earlier deterministic model of Hunderi et al. (1979). These authors pointed out that the statistical theories described in §11.2.3 do not allow for the fact that a grain of a particular size can grow in an environment where it is surrounded by smaller grains, but will shrink if surrounded by larger grains, i.e. R_{crit} in equation 11.13 varies with position. They proposed a **linear bubble model** in which a bubble **i** makes contact with a number of other bubbles $\mathbf{i-n}$ to $\mathbf{i+n}$, where **n** depends on the relative sizes of the bubbles. The pressure difference between bubbles of different sizes leads to the transfer of material between the bubbles and sets of coupled equations are solved to predict the size distribution and grain growth kinetics of the bubbles, which are found to be close to those for parabolic growth predicted by Hillert. Extension of such an analytical model to large numbers of grains in 3-D is however, not currently practicable. The most promising deterministic models of grain growth in recent years have been those based on computer simulation of grain growth using the **equation of motion** and **Monte-Carlo** simulation methods, details of which are discussed in §16.2.

11.2.4.1 Equation-of-motion computer simulation

In this approach, which has mainly been applied to 2-D at present, a starting grain structure is specified, and this microstructure is then allowed to equilibrate by allowing the boundaries and vertices to move according to specific equations. For example, a boundary is adjusted to allow the angles at the triple points to be 120° and then the boundary is allowed to move by an amount proportional to its radius of curvature, this cycle being repeated over all boundaries a large number of times. This is essentially a quantification of the logical arguments which suggested the sequence shown in figure 11.4. The key feature of this type of approach is that once the initial microstructure is

constructed, the laws of motion formulated, and procedures for dealing with vertex contact and grain switching (fig. 16.8) specified, then no further assumptions are needed regarding topology, and the grain growth behaviour is thus truly deterministic.

A number of different authors have developed **vertex models** based on such methods (§16.2.4), and these are reviewed by Anderson (1986) and Atkinson (1988). The slightly different physical principles used have resulted in rather different grain size distributions and growth kinetics, although the latter are generally close to parabolic. These simulations have also shown that the initial growth kinetics are very sensitive to the starting grain structure. In order to make a significant contribution to our understanding of grain growth, this approach needs to be developed in 3-D, and preliminary work in this area has been carried out Nagai et al. (1992) and Maurice (2000).

11.2.4.2 Monte-Carlo computer simulation

The Monte-Carlo simulation technique, the principles of which are discussed in §16.2.1, has been extensively used to study grain growth. Early tests of a 2-D model (Anderson et al. 1984) showed that the shrinkage of a large isolated grain of area **A**, followed the relationship

$$A - A_0 = -ct \tag{11.25}$$

where A_0 is the grain size at $t = 0$ and c is a constant.

This leads to a parabolic relationship between grain size and time similar to that predicted by many theories (equation 11.5) and shows that the simulation leads to a linear dependence of boundary velocity on driving pressure (i.e. equation 5.1).

Significantly however, the growth of a 2-D grain structure such as is shown in figure 16.4, was found after an initial transient, to give a grain growth exponent of **2.44.** This differed significantly from the value of **2** predicted by the statistical theories discussed in §11.2, and was closer to the experimentally measured values (tables 11.1 and 11.2). Analysis of the computer-generated microstructures suggested that deviation from the exponent of 2 was due to topological effects. In particular, the movement and rotation of vertices was found to result in the redistribution of curvature between adjacent boundaries, and it was suggested by Anderson et al. (1984) that this lowered the local driving pressures for boundary migration, and was responsible for the higher grain growth exponent. These simulations indicated the importance of the random motion of boundaries which was first considered by Louat (1974) and also emphasised the importance of the local environment of a grain. Extension of these simulations to 3-D (Anderson et al. 1985) resulted in a grain growth exponent of **2.81** as compared to the Rhines and Craig (1974) prediction of **3.** At the time, these results therefore supported the Rhines and Craig (1974) view that grain growth exponents larger than **2** were an inevitable consequence of topological factors.

However, later simulations by the same group (Anderson et al. 1989a) run for longer times with larger arrays indicated that the earlier results were incorrect as they **did not represent steady state grain growth and were influenced by the starting grain structure.** The later

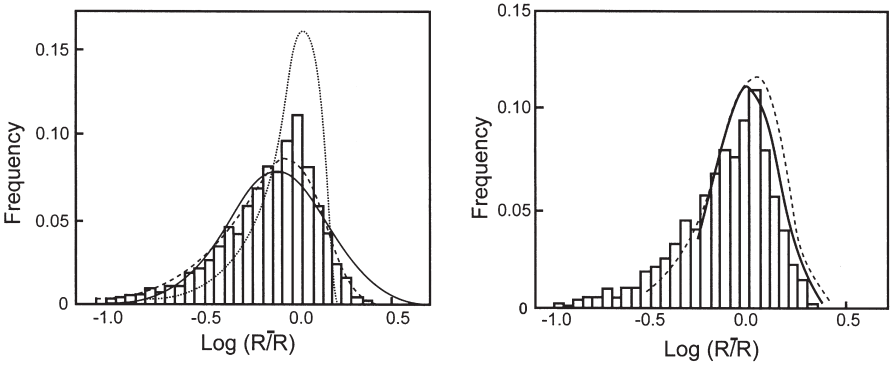

Fig. 11.6. Histogram of the grain size distributions from 2-D Monte-Carlo simulations compared with: (a) Theoretical distributions - log-normal (Feltham 1957), Hillert (1965) dotted, and Rayleigh (Louat 1974) dashed, (b) Experimental data - for aluminium (Beck 1954) and MgO (Aboav and Langdon 1969), dashed line, (after Srolovitz 1984a).

results revealed a growth exponent of **2.04** in 2-D and **2.12** for a 3-D simulation, which are very close to the $\mathbf{n = 2}$ parabolic kinetics which are predicted on most theories, and Anderson concluded that the asymptotic long-time growth exponent is **2.**

The grain size distributions obtained by the Monte-Carlo simulations have been analysed by Srolovitz et al. (1984a) and Anderson et al. (1989a). The grain size distribution function, expressed in terms of $R/\bar{R}$ is found to be time invariant and close to experimental measurements as shown in figure 11.6. The grain size distribution determined from 2-D sections of the 3-D grain structure is closest to the Rayleigh distribution suggested by Louat (1974).

11.2.5 Recent theoretical developments

As noted in §11.1.1, modelling of grain growth remains a remarkably active area, and over the past decade over 20 papers have, on average, been published annually, most of these being refinements of earlier models. The mean field approach has been improved by taking account of spatial correlation among grains of different sizes (Marthinsen et al. 1996), and whilst this gives the correct kinetics, the size distributions are not in agreement with experiment unless further modifications are made (Mullins 1998a). Stochastic theories, often using the Fokker–Planck formulation, are based on a given grain growing in an environment which varies from grain to grain, and this gives a more complete description of grain growth (Mullins 1998a,b, Pande and Rajagopal 2001). However, a universally accepted stochastic theory of coarsening is not yet available (Pande and Rajagopal 2001). Models which take into account the fact that the grain boundary energies and mobilities in real materials are not isotropic have also been formulated (Kazaryan et al. 2002).

11.2.6 Which theory best accounts for grain growth in an ideal material?

The question should now be considered as to which theory or model, if any, is close to accounting for grain growth in pure single-phase materials. That there is no obvious answer is clear from the large number of approaches that are actively being pursued. Ryum and Hunderi (1989) have given a very clear analysis of the statistical theories of grain growth and shown that all make questionable assumptions.

We will briefly consider a number of basic questions:

(i) Is a grain growth exponent of 2 inevitable?
The discussions in this section have shown that the vast majority of theories predict parabolic kinetics. The main dissent from this is the work of Rhines and Craig (1974) which predicted $\mathbf{n = 3}$**.** However, their analysis is no longer accepted, and the extension of their work by Kurtz and Carpay (1980) predicted $\mathbf{n = 2}$**.** Indications from early Monte-Carlo simulations that a higher value of n was associated with topographic factors (Anderson et al. 1984) have proved to be an artefact of the model, as later simulations (Anderson et al. 1989a) found $n \sim 2$. In a review of the theory of the coarsening behaviour of **statistically self similar structures,** i.e. those in which the structure remains geometrically similar in a statistical sense, Mullins and Vinals (1989) concluded that for curvature driven growth, such as occurs during grain growth, an exponent of $\mathbf{n = 2}$ is inevitable.

The evidence in favour of $n = 2$ being the prediction of theory for an ideal single-phase material in which the boundary velocity is proportional to driving pressure and boundary energies are isotropic, appears to be conclusive.

(ii) Can grain size distributions be used to prove or disprove a theory?
As discussed earlier in this section, the various theories predict different grain size distributions, although it is usually predicted that the grain size distribution expressed in terms of normalised grain size ($R/\bar{R}$) will remain invariant during growth.

As shown in figure 11.6, the experimental data appear to be closest to the Rayleigh distribution, with the narrow Hillert distribution giving the worst fit. More recent reviews of experimental distributions (Pande 1987, Louat et al. 1992) have confirmed this, and the results of later Monte-Carlo simulations (Anderson et al. 1989a) have produced data consistent with the Rayleigh distributions. In comparing experiment with theory it should be noted that as discussed in §11.2.3.2, measurements from 2-D sections will only reflect the 3-D grain distribution if the grain structure is isotropic. Although there have been numerous correlations of measured and predicted distributions, Frost (1992) has shown that the grain size distribution predicted by individual statistical models can be varied by very small adjustments to the models and cannot therefore be used to prove the validity of a model.

(iii) Why is a grain growth exponent of 2 rarely measured?
As discussed in §11.1.4 and summarised in tables 11.1 and 11.2, grain growth exponents of **2** are rarely found experimentally and average values are close to **2.4.** If we accept that theory predicts $\mathbf{n = 2}$**,** then we must conclude that **the larger measured exponents are a consequence of the materials used not being ideal** i.e. not consistent with the basic

assumptions about the material which are incorporated in the models. We should recall that the driving pressure for grain growth is very small (§11.1) and therefore any small deviations from an 'ideal material' may have a very large effect on kinetics. There are several important parameters of the material which may lead to loss of ideality and have an influence on the kinetics:

- **The initial grain structure is not equiaxed or is far from the steady state grain size distribution.** Changes in grain size distribution during growth are known to affect experimentally measured grain growth kinetics (e.g. Takayama et al. 1992, Matsuura and Itoh 1992) and have been shown to produce large exponents during the early stages of growth in Monte-Carlo simulations (Anderson et al. 1984, 1989a).
- **The presence or development of a texture.** This would result in the occurrence of non-uniform boundary energies and mobilities thereby invalidating equations 11.3 and 11.4 which form the basis of grain growth theory.
- **The presence of very small amounts of a second-phase or other pinning defect.** As discussed in §11.1.4 this could account for high values of **n.**

These last two important factors are considered in more detail in the following sections.

11.3 GRAIN ORIENTATION AND TEXTURE EFFECTS IN GRAIN GROWTH

11.3.1 Kinetics

11.3.1.1 Experimental measurements

The rate of grain growth may be affected by the presence of a strong crystallographic texture (Beck and Sperry 1949). This arises at least in part from a large number of grains of similar orientation leading to more low angle (i.e. low energy and low mobility) boundaries (§4.2). Thus the driving pressure (equation 11.3) and hence the rates of growth are reduced. The texture may also alter during grain growth thereby affecting the kinetics (Distl et al. 1982, Heckelmann et al. 1992). The evolution of textures during grain growth is discussed in §12.4.4, and an example of the complex grain growth kinetics which are found when there are concurrent texture changes is seen in figure 12.22b.

11.3.1.2 Theories

Novikov (1979) modified a statistical model of grain growth to include variations of boundary energy and showed how the presence of texture would affect the kinetics of grain growth. Abbruzzese and Lücke (1986) and Eichelkraut et al. (1988) have incorporated the effects of texture into Hillert's model of grain growth. They argued that if a material contained texture components A,B,C ... etc., then the uniform boundary energies (γ_b) and mobilities (M) in equations 11.13 and 11.14 should be replaced by specific values relating to the texture components, ($\gamma_b{}^{AB}$, M^{AB} etc.) and that the critical radius R_{crit} in equation 11.13 would be different for each group of boundaries. They then calculated the grain growth of each texture component and showed that this might have a very strong effect on the grain size distribution and growth kinetics. Figure 11.7 shows the predicted change in these parameters for a material containing two texture components, A and B. The initial relative mean grain

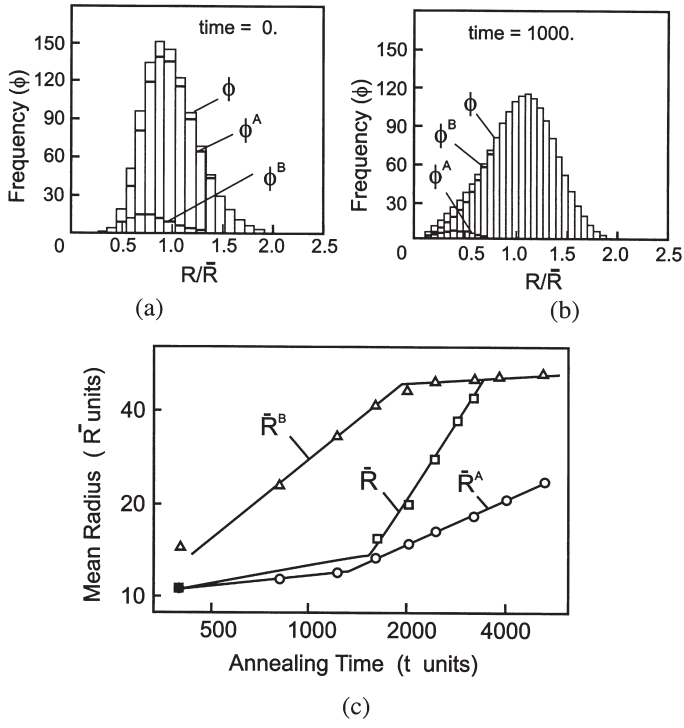

Fig. 11.7. Predicted grain growth in a microstructure containing texture components A and B. (a) Initial grain size distribution, (b) Grain size distribution after growth, (c) Growth kinetics, (after Abbruzzese and Lücke 1986).

sizes are $\bar{R}_B/\bar{R}_A = 0.8$, and the mobilities are $M^{AB}/M^{AA} = 5$ i.e. the mobility of A grains growing into B grains is five times that of A grains growing into A. It may be seen that in this case the A component is strongly depleted during growth (fig. 11.7a,b), that the grain size distribution is drastically altered, and that the relationship between $\bar{R}$ and t is complex (fig. 11.7c). There is some evidence of agreement between the predictions of the model and experimental measurements (Abbruzzese and Lücke 1986), although too much reliance should not be placed on quantitative agreement because the relationships between the mobility, energy and misorientation of grain boundaries are not known accurately.

11.3.1.3 Computer modelling

Grest et al. (1985) extended their Monte-Carlo simulation studies of grain growth to include variable boundary energies. They set the boundary energies according to the Read–Shockley relationship (equation 4.6) and varied the energy range by altering θ_m, the angle at which the energies saturate according to this equation. The simulation is therefore close to representing the annealing behaviour of a microstructure comprising a mixture of both high angle and low angle boundaries. However, as the mobilities of the

boundaries were not varied, the low angle (low energy) boundaries did not have the correspondingly low mobilities expected in a real material (§5.2). They found that the introduction of variable boundary energy led to an increase in the growth exponent (**n**) to **4.** The number of low angle boundaries increased during the anneal, compared with the constant energy simulation and the grain size distribution was broader. This simulation may be compared with the vertex simulation of recovery shown in figure 6.19, in which the low angle boundaries had both low energies and low mobilities and in which a large growth exponent **n** and a decrease in boundary misorientation were also found.

11.3.2 The effect of grain growth on grain boundary character distribution

As automated techniques for the rapid determination of crystallite orientations have become widely available in recent years, there has been a growing interest in the effect of grain growth and other annealing processes on **grain boundary character,** and particularly on its **distribution (GBCD),** (e.g. figs. 4.2 and A2.1) which is as much a quantitative measure of the microstructure of a material as is the grain size.

11.3.2.1 The frequency of special boundaries

There is a large body of evidence to show that the relative fractions of low-Σ boundaries often change during grain growth. In metals of medium to low stacking fault energy, where significant numbers of $\Sigma 3^n$ boundaries are present, the populations of both these and $\Sigma 1$ boundaries tend to increase during grain growth. Thus, in nickel, Furley and Randle (1991) reported an increase in $\Sigma 3$ (twin) boundaries and a decrease in $\Sigma 5$ boundaries during grain growth, and Randle and Brown (1989) found an increase in both low angle ($\Sigma 1$) and other low Σ boundaries during the annealing of austenitic stainless steel. Pan and Adams (1994) reported a greatly increased number of special boundaries ($\Sigma 1$, $\Sigma 3$ and $\Sigma 9$) during grain growth of Inconel 699.

Some of the clearest evidence as to the change of boundary character during grain growth in such materials has been obtained by Watanabe et al. (1989) who examined the misorientations of boundaries after grain growth and abnormal grain growth in an Fe–6.5%Si alloy which was annealed after rapid solidification. After a short annealing time (fig. 11.8a) the distribution of misorientation is close to the random value (fig. 4.2), but at long times (fig. 11.8c) it shifts markedly towards lower misorientations and a strong {100} texture develops. The frequency of low Σ and low angle boundaries was also found to increase markedly as grain growth proceeded as shown in figure 11.8d.

In fcc metals of high stacking fault energy, where there are few $\Sigma 3$ boundaries, but in which there are low angle ($\Sigma 1$) boundaries, the mean misorientation and therefore energy of these boundaries has been shown to decrease during subgrain growth when there is no orientation gradient, as discussed in §6.5.2.1 and shown in figure 6.16b.

11.3.2.2 Interpretation of the data

It was argued in §6.5.3.4 that the annealing of a microstructure with a distribution of boundary energies, the boundary tensions would inevitably lead to a decrease in the

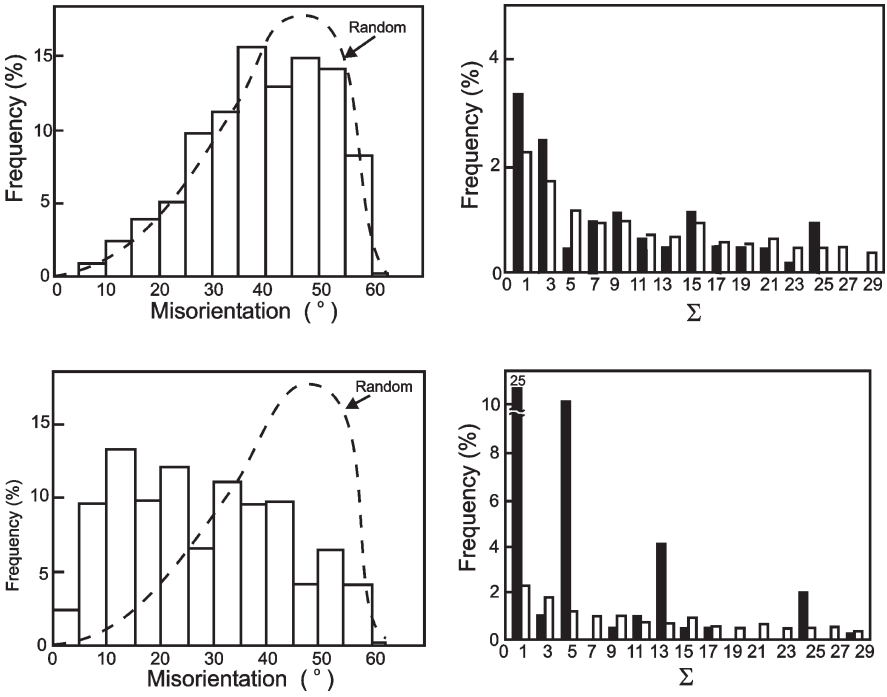

Fig. 11.8. The effect of grain growth on grain boundary character in rapidly solidified Fe–6.5wt%Si. (a) After an anneal for 600 secs at 1090°C, the measured distribution of grain misorientations is close to that for randomly oriented grains, and, (b) the frequency of special boundaries (shaded) is close to the random value (open), (c) After annealing for 3500 at 1090°C the mean misorientation is reduced and, (d) the frequency of low angle (Σ1) and other special boundaries is increased, (after Watanabe 1989).

total amount of high energy boundary relative to low energy boundary. This has been observed as discussed above, and has been shown to occur in both Monte-Carlo (Grest et al. 1985, Holm et al. 2001) and vertex (Humphreys 1992b) computer simulations.

In order to illustrate semi-quantitatively, the complexities of the problem we have run a simple vertex simulation with an initial microstructure containing five generic types of grain boundary:

1. Random high angle boundaries of constant energy and mobility
2. Low energy boundaries with low mobility (typified by LAGBs or Σ3 twins)
3. Low energy boundaries with high mobility (typified by low Σ boundaries in pure metals)
4. High energy boundaries with low mobility
5. High energy boundaries with high mobility

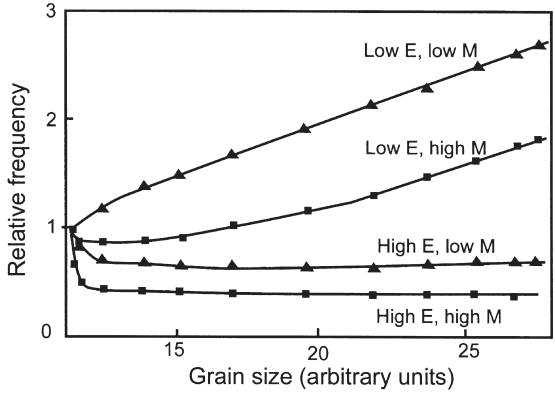

Fig. 11.9. Computer simulation of the change in boundary type during grain growth. The boundary frequencies are expressed as multiples of the frequency of a 'random' boundary.

High or low energies or mobilities were given values of x5 or 1/5 respectively that of the random boundaries. It was found that the distribution of boundary types changed during grain growth as shown in figure 11.9.

It is seen that there is a tendency for the proportion of low energy boundaries to increase and for high energy boundaries to decrease during grain growth. However, the boundary mobility plays a significant role, and it is interesting that the largest increase is predicted for low energy/low mobility boundaries such as LAGBs ($\Sigma 1$) and other low-Σ boundaries, which is in accord with the experimental results of figure 11.8.

From the above considerations of the effects of grain orientation and boundary character on grain growth, we conclude that there is experimental and theoretical evidence that bulk and local orientation effects are important during grain growth, and that these affect both the kinetics of grain growth and the microstructure. There is growing evidence that the **ideal materials with isotropic and unchanging boundary energy which are addressed in the standard theories of grain growth simply do not exist,** and the most fruitful developments in the theory of grain growth in single-phase materials will be those which take a more realistic account of orientation effects during grain growth.

11.3.2.3 Grain boundary engineering

The grain boundary character distribution can be of industrial significance because certain mechanical and physical properties of polycrystals depend on the nature of the grain boundaries. It has long been known that the properties of low energy low Σ boundaries differ from those of more general or 'random' high angle boundaries (e.g. §5.3.2), and it is well established (e.g. Palumbo and Aust 1992, Aust et al. 1993, Watanabe 1998) that the presence of such boundaries may improve the engineering

performance of the material. Important properties of such boundaries may include:

- Lower rates of grain boundary sliding during creep.
- Resistance to high temperature fracture.
- Resistance to solute segregation, precipitation and intergranular embrittlement.
- Lower electrical resistivity.
- Resistance to corrosion.
- Resistance to stress corrosion.

It was first suggested by Watanabe (1984) that thermomechanical processing could be used to control grain boundary distributions so as to improve the properties of materials, and this has given rise to the concept of **grain boundary engineering (GBE),** which is currently a very active research area, particularly for metals of medium and low stacking fault energy (see e.g. Watanabe 1998). GBE has been successfully exploited commercially in areas including the improvement in service performance of austenitic stainless steels and nickel alloys in power plant by Ontario Hydro (Lehockey et al. 1998), and an improvement in the corrosion and creep resistance of lead-acid battery grids (Lehockey et al. 1999).

Both recrystallization and grain growth may be used to increase the fraction of low Σ boundaries, and many cycles of deformation and annealing are often employed in order to optimise the material. For many applications, it is not simply the number of low energy boundaries which is important, but also their spatial distribution. For example, if failure occurs along grain boundaries of 'random' character, then it is important that the low-Σ boundaries are situated so as to break up the network of these boundaries. Thus the **3-dimensional connectivity of the boundaries** is also an important parameter (Randle 1999, Kumar et al. 2002, Schuh et al. 2003).

The science underlying the thermomechanical processing schedules used in grain boundary engineering is surprisingly poorly understood, and most of the processing schedules, some of which are patented, are purely empirical. In order to establish scientifically-based methods for controlling the boundary character distributions, there is a need for systematic research to establish how and why **recrystallization** affects the number and distribution of special boundaries. The effect of **grain growth** on the number of special boundaries is more predictable as discussed in §11.3.2.2 and shown in figures 11.8 and 11.9, although more detailed quantitative models are required.

11.4 THE EFFECT OF SECOND-PHASE PARTICLES ON GRAIN GROWTH

It was shown in §4.6 that second-phase particles exert a strong pinning effect (**Zener pinning**) on boundaries, with the pinning pressure being determined primarily by the size, volume fraction, interface and distribution of the particles. Because the driving pressure for grain growth is extremely low, particles may have a very large influence both on the kinetics of grain growth and on the resultant microstructures. It should be noted that at the high temperatures at which grain growth occurs, the dispersion of second-phase particles may not be stable. We will first deal with the behaviour of a material containing a stable dispersion of particles and at the end of this section

consider the cases where the particles themselves form, coarsen or migrate during the process of grain growth. It should be noted that the quantitative relationships presented below are based on the interaction of boundaries with a random distribution of non-coherent equiaxed particles. For other types of particle the retarding pressure due to the particles may be different as discussed in §4.6.1 and appropriate modifications to the theory should therefore be made.

Although the discussion below is presented in terms of **normal grain growth,** many of the considerations are also relevant to the **growth of a subgrain structure during recovery.** Those aspects of the theory which are particularly relevant to subgrain growth are further discussed in §6.6.

11.4.1 Kinetics

A dispersion of stable second-phase particles will reduce the rate of grain growth because the driving pressure for growth (P in equation 11.3) is opposed by the pinning pressure (P_z) due to the particles (equation 4.24). If this is incorporated into a simple grain growth theory such as the Burke and Turnbull (1952) analysis (§11.1.3), the rate of grain growth becomes

$$\frac{dR}{dt} = M(P - P_z) = M\left(\frac{\alpha\gamma_b}{R} - \frac{3F_v\gamma_b}{2r}\right) \tag{11.26}$$

This predicts a growth rate which is initially parabolic, but which subsequently reduces and eventually stagnates when $P = P_Z$.

Hillert (1965) extended his theory of normal grain growth to include the effects of particle pinning on the kinetics of grain growth and on the grain size distribution. The pinning pressure due to the particles results in a modification to the growth rate for single-phase materials (equation 11.13)

$$\frac{dR}{dt} = cm\gamma_b\left(\frac{1}{R_{crit}} - \frac{1}{R} \pm \frac{z}{c}\right) \tag{11.27}$$

where $c = 0.5$ for 2-D and 1 for 3-D and $z = 3F_V/4r$

For grains in the size range $1/R \pm z/c$, the net pressure for boundary migration will be zero and therefore no growth or shrinkage will occur. Grains larger or smaller than this will shrink or grow at a reduced rate. Hillert suggests that the mean growth rate will be given by

$$\frac{d\bar{R}^2}{dt} = \frac{cM\gamma_b}{2}\left(1 - \frac{z\bar{R}}{c}\right)^2 \tag{11.28}$$

which predicts a more gradual retardation of growth rate than equation 11.26. Hillert (1965) also points out that the grain size distribution will be affected by particle pinning. Abbruzzese and Lücke (1992) have extended this model and showed that the width of

the grain size distribution during normal grain growth should be reduced by particle pinning, for which there is some experimental evidence (Tweed et al. 1982).

11.4.2 The particle-limited grain size

It was shown many years ago by Zener (1948) that when the pressure on a boundary due to particle pinning equalled the driving pressure for grain growth, growth would cease and a **limiting** grain size would be reached. The existence of a limiting grain size is of great practical importance in preventing grain growth during the heat treatment of industrial alloys.

11.4.2.1 The Zener limit

In the situation which was first considered by Zener, the grain boundary is considered to be macroscopically planar as it interacts with the particles and therefore the pinning pressure (P_z) is given by equation 4.24. The driving pressure for growth (P) arises from the curvature of the grain boundaries, and is given by equation 11.3. Grain growth will cease when $P = P_z$. i.e.

$$\frac{\alpha \gamma_b}{R} = \frac{3 F_v \gamma_b}{2r} \tag{11.29}$$

If the mean grain radius is taken to equal the mean radius of curvature (R) then we obtain a limiting grain size

$$D_z = \frac{4\alpha r}{3F_V} \tag{11.30}$$

Setting $\alpha = 1$ (some authors use other values), results in the well known **Zener limiting grain size**

$$D_{Zener} = \frac{4r}{3F_V} \tag{11.31}$$

It has long been recognised that this is only an approximate solution, and numerous alternative approaches have been attempted. Hillert (1965) derived a limiting grain size from equation 11.27 by equating $1/R_{crit}$ with z/c for the case when R is large, giving a limiting grain radius for the 3-D analysis, of $4r/3F_V$, i.e. a grain diameter of twice that of equation 11.31 (α in equation 11.30 equal to 0.5). Gladman (1966) developed a geometric model consisting of tetrakaidecahedral grains and considered the effect of particles on the growth and shrinkage of the grains. He concluded that the limiting grain size was given by

$$D_G = \frac{\pi r}{3F_V}\left(\frac{3}{2} - \frac{2}{Z}\right) \tag{11.32}$$

where Z is the ratio of the maximum grain size to the average grain size, a parameter which is not readily calculated, but which is expected to lie between 1.33 and 2. Hillert's

(1965) grain growth theory gives $Z = 1.6$, and Gladman has suggested $Z = 2$. Using this value, Gladman's model, which has the same dependence on F_V and r as equation 11.30, predicts a limiting grain size which is smaller than that of equation 11.31, corresponding to equation 11.30 with $\alpha = 0.375$.

Numerous refinements to the Zener treatment have been carried out (e.g. Louat 1982, Hellman and Hillert 1975, Hillert 1988) and **these generally predict a limiting grain size which is of a similar form to equation 11.30 with $0.25 < \alpha < 0.5$,** i.e. considerably smaller than that predicted by equation 11.31. The many refinements of the Zener relationship have been comprehensively reviewed by Manohar et al. (1998).

11.4.2.2 Comparison with experiment

There are surprisingly few experimental results available to test these relationships accurately in materials containing low volume fractions of particles, and in particular to verify the dependence of D_Z on F_V. Gladman (1980) compared measurements of the limiting grain size (D_Z) from a number of investigations with his theory and found reasonable agreement. Tweed et al. (1982) in a detailed study of the recrystallized grain sizes and size distributions in three aluminium alloys containing very low volume fractions of Al_2O_3, found limiting grain sizes which in some cases corresponded to very small values of α in equation 11.30. However the data showed considerable scatter and it is difficult to reconcile the trend of the data with any model of limiting grain size. The limiting grain sizes obtained by Koul and Pickering (1982) after grain growth of iron alloys containing volume fractions of $\sim 5 \times 10^{-3}$ of carbide particles are shown in figure 11.10. It may be seen that although the data are limited and scattered, there is fair agreement with the theoretical line corresponding to equation 11.30 with $\alpha = 0.37$, i.e. Gladman's model. Manohar et al. (1998) have analysed the available experimental results for iron and aluminium alloys containing small volume fractions of second-phase particles, and conclude that they are consistent with equation 11.30 with $\alpha \sim \mathbf{0.26}$ (see fig. 11.12).

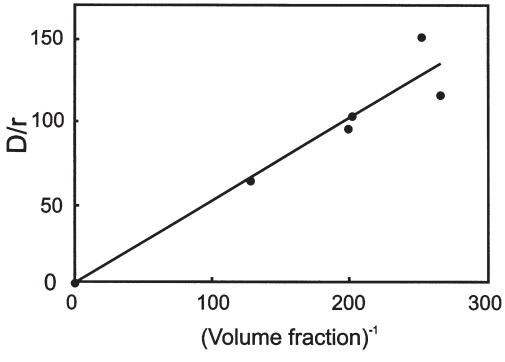

Fig. 11.10. The particle-limited grain size in carbide-containing Fe–Ni–Cr alloys, (data from Koul and Pickering 1982).

11.4.2.3 Particle-boundary correlation effects

The analyses discussed in §11.4.2.1 assumed that the pinning pressure (P_z) was that for a macroscopically planar boundary. However, as discussed in §4.6.2.2, when the interparticle spacing is similar to the grain size, this assumption is not valid, and non-random correlation of particles and boundaries must be taken into account. This will be particularly important in materials with large volume fractions of particles. In this situation, a limiting grain size (D_{Z1}) is found by equating the driving pressure (equation 11.3) with the pinning pressure as given by equation 4.27.

$$D_{Z1} = r\left(\frac{8\alpha}{3F_V}\right)^{1/2} \approx \frac{1.6\alpha^{1/2}r}{F_V^{1/2}} \tag{11.33}$$

The limiting grain size given by equation 11.33 is very similar to that suggested by Anand and Gurland (1975) for subgrain growth (fig. 6.29 and §6.6.2.1). It is however likely that D_{Z1} which represents the situation when all particles are on boundary corners but not all boundary corners are occupied by particles (fig. 4.25a), represents a lower bound for the limiting grain size and that grain growth will actually continue to occur until all grain corners are pinned, i.e. the grain size D_C of equation 4.28 (fig. 4.25b).

$$D_{ZC} = D_C \approx N_V^{-1/3} \approx \frac{\beta r}{F_V^{1/3}} \tag{11.34}$$

where β is a small geometric constant.

Various authors (Hellman and Hillert 1975, Hillert 1988, Hunderi and Ryum 1992a) have discussed this type of relationship, and Hillert (1988) suggests that $\beta = 3.6$.

The experimental measurements of limiting grain size in alloys containing large volume fractions of particles ($F_V > 0.05$) are very scattered (Hazzledine and Oldershaw 1990, Olgaard and Evans 1986) and although there is some indication that the limiting grain size is inversely proportional to F_V^n, where $n < 1$, the results are by no means conclusive. If equation 11.34 is assumed to hold, then analyses of the results of Hellmann and Hillert (1975) on steels and the data for Al–Ni of figure 11.14 give β as 3.3 and 3.4, respectively. The subgrain data of Anand and Gurland (1975) which were analysed by them in terms of equation 11.33 also fit equation 11.34, as shown in figure 6.29, with $\beta = 2.7$.

Figure 11.11 shows the predicted variation of the limiting grain sizes D_Z and D_{ZC} with volume fraction according to equations 11.30 and 11.34 using values of the geometric constants ($\alpha = 0.35$, $\beta = 3$) which are consistent with experiment. It may be seen that the curves cross at a volume fraction of ~0.06. At volume fractions less than this the particle-correlated limit (D_{ZC}) is unstable with respect to growth, and the uncorrelated limit (D_Z) is appropriate, whereas at higher volume fractions the limit will be D_{ZC}. In practice there will be a gradual transition between correlated and uncorrelated pinning as considered in §4.6.2.2, and this has been discussed by Hunderi and Ryum (1992a). The actual volume fraction at which the transition from D_Z to D_{ZC} occurs is not yet firmly established either theoretically or experimentally, but theoretical estimates

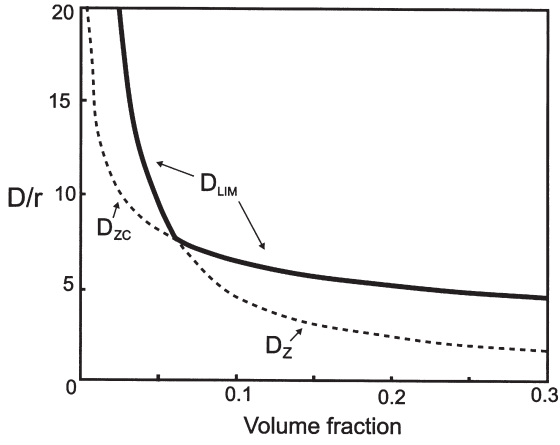

Fig. 11.11. The predicted variation with particle size and volume fraction of the particle-boundary correlated limiting grain size (D_{ZC}) for $\beta = 0.3$, and the non-correlated limiting grain size (D_Z) for $\alpha = 0.35$.

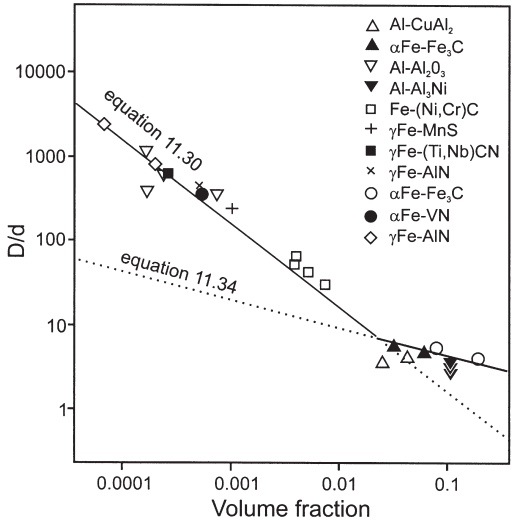

Fig. 11.12. Experimental measurements of the limiting grain/particle size ratio as a function of the volume fraction. The result are consistent with a transition from a F_V^{-1} to a $F_V^{-1/3}$ relationship at a volume fraction of ~0.05, in agreement with the theoretical analysis of figure 11.11, (after Manohar et al. 1998).

(Hillert 1988, Hazzledine and Oldershaw 1990, Hunderi & Ryum 1992a) put it within the range $0.01 < F_V < 0.1$, which is consistent with figure 11.11. A recent analysis by Manohar et al. (1998) of several experimental investigations, is shown in figure 11.12. The experimental results are seen to be consistent with the analysis of figure 11.11,

suggesting a transition from a F_V^{-1} to a $F_V^{-1/3}$ dependence of the limiting grain size, at $F_V \sim 0.05$.

The above considerations suggest that the effective limiting grain size (D_{lim}), will be the larger of D_Z or D_{ZC}, the solid line in figure 11.11, and that the transition will occur at a volume fraction of ~0.05.

11.4.2.4 Computer simulations

Extensive computer simulation of particle-controlled grain growth has been carried out using the Monte-Carlo technique (§16.2.1). The initial work (Srolovitz et al. 1984b) which was a 2-D simulation found a limiting grain size proportional to $F_V^{-1/2}$. However, it has since been shown (Hillert 1988, Hazzeldine and Oldershaw 1990) that the situation in 3-D is quite different and that the **2-D simulations of particle-limited grain growth are not applicable to grain growth in a 3-D microstructure, because a particle in a 2-D simulation is equivalent to a fibre in 3-D!** Later three dimensional Monte-Carlo simulations (Anderson et al. 1989b, Hazzledine and Oldershaw 1990) found a limiting grain size in accordance with equation 11.34, although their value of β (~9) is considerably larger than that found experimentally (§11.4.2.3). The earlier 3-D Monte-Carlo simulations were often limited to a lattice of $\sim 100^3$ units, with a particle diameter equal to one unit. Therefore for volume fractions less than ~0.05, as may be seen from equation 11.34, the limiting grain size approaches the size of the array, and accurate results cannot be obtained. Such simulations were therefore limited to the range in which D_{ZC} is expected to apply and could neither verify nor contradict the prediction that the limiting grain size (D_{lim}) changes from D_Z to D_{ZC} at a critical volume fraction.

Recent larger scale Monte Carlo simulations (Miodownic et al. 2000) have shown a F_V^{-1} dependence of the limiting grain size, in agreement with the original Zener prediction of equation 11.30, with $\alpha \sim 1$, i.e. equation 11.31, for particle volume fractions in the range 0.025 to 0.15. However, there are only 4 data points, and these results contradict the analytical considerations, other simulations and experiments discussed above, inasmuch as they find no transition at high volume fraction to a $D \propto F_V^{-1/3}$.

Although there is now more general agreement that at low volume fractions, the Zener relationship of equation 11.30 is obeyed, **the question of the transition to a relationship such as equation 11.34 at large volume fractions, remains unclear, requiring further investigation.**

11.4.2.5 A solute limited grain size?

As discussed in earlier sections, grain growth is promoted by the reduction in energy (ΔE_B) as the area of grain boundary decreases during growth. However for a solid solution, the situation is more complicated because some of the solute will segregate to the boundaries and lower the specific boundary energy (§5.4.2) whilst the remaining solute will raise the energy of the material in the grain interior (ΔE_G).

Consider a small-grained polycrystal containing a small amount of a solute which segregates strongly to the boundaries (see fig. 5.30). Initially, most of the solute will be in the grain boundaries. However, as the grains grow, the boundary area becomes

insufficient to accommodate all the solute, and some will be rejected, raising the free energy of the grain interiors.

At some stage of growth, the net free energy change, ΔE_G-ΔE_B, may become positive and the driving force for grain growth vanishes, i.e. we have a limiting grain size which is determined by solute. Such a concept was proposed by Weissmuller (1993) as being a method of promoting grain stability in nanostructured materials. The theory was further examined by Kirchheim (2002), who claimed that it would account for the stability of nano-scale grains in Ni–P and Ru–Al alloys, and has also been discussed by Gleiter (2000) in his review of nanostructured materials. The somewhat similar case of vacancy-limited grain growth is discussed in §5.3.4.1.

11.4.3 Particle instability during grain growth

We have assumed so far, that the second-phase particles are stable during grain growth. There are many situations in which this is not so, and in this section we examine the consequences of instability of the second-phase during grain growth for three important cases.

11.4.3.1 Precipitation after grain or subgrain formation

In some situations the second-phase particles may be precipitated after the formation of a grain or subgrain structure. In this case the particles are unlikely to be distributed uniformly and will form preferentially on the boundaries. The pinning pressure due to the particles will therefore be greater than for a random particle distribution (Hutchinson and Duggan 1978) as discussed in §4.6.2.3. If it is assumed that all the particles are on boundaries and are randomly distributed on these boundaries, then the pinning pressure is given by equation 4.36 and by equating this with the driving pressure given by equation 11.3, the limiting grain size is

$$D_{ZP} = r\left(\frac{8\alpha}{F_V}\right)^{1/2} \tag{11.35}$$

It is expected that in practice this situation will be more applicable to the **growth of subgrains during recovery** (§6.6) than to **grain growth,** although no quantitative tests of equation 11.35 have yet been reported.

11.4.3.2 Coarsening of dispersed particles during grain growth

An important situation is one in which grain growth has stagnated due to the particle dispersion, but the particles coarsen (Ostwald ripening). In this situation the grain size (D) is equal to D_{lim} as defined in §11.4.2.3, and the rate of growth is controlled by the rate of change of particle size. Thus

$$\frac{dR}{dt} = c\frac{dr}{dt} \tag{11.36}$$

where the constant c is $2\alpha/3F_V$ for low volume fractions and $\beta/2F_V^{1/3}$ for large volume fractions.

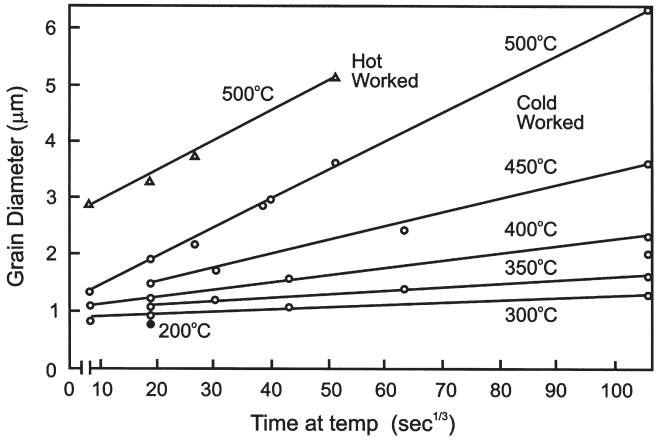

Fig. 11.13. The kinetics of grain growth when controlled by particle coarsening for an Al–6wt%Ni alloy containing a volume fraction of 0.10 of $NiAl_3$ particles, (Morris 1976).

The rate of particle coarsening will depend on the rate controlling mechanism (Hillert 1965, Gladman 1966, Hornbogen and Koster 1978, Ardell 1972, Martin and Doherty 1976). If the particle growth is controlled by volume diffusion (diffusivity $= D_s$) then (Wagner 1961)

$$\bar{R}^3 - \bar{R}_0^3 = c_1 D_s t \tag{11.37}$$

whereas for particle growth controlled by diffusion along the grain boundaries (diffusivity $= D_b$), which is commonly found for large volume fractions, as discussed below, then

$$\bar{R}^4 - \bar{R}_0^4 = c_2 D_b t \tag{11.38}$$

Figure 11.13 shows the kinetics of grain growth in an Al–6wt%Ni alloy which contains a volume fraction of 0.1 of $NiAl_3$ particles of initial diameter 0.3 μm. The grain growth kinetics, which are controlled by the particle coarsening are seen to be in accord with equation 11.37 over a wide temperature range. Figure 11.14 shows the relationship between the size of the grains and the second-phase particles in the same alloy system. The grain size is found to be proportional to the particle size as would be predicted by equation 11.34. From the slope of the line, the constant β in the equation is found to be 3.4. A similar linear relationship between particle and subgrain size has been reported in a commercial Al–Fe alloy (Forbord et al. 1997).

Coarsening of the particles by grain boundary diffusion will of course only affect those particles which are on grain boundaries, and other particles will coarsen more slowly. However, as grain growth occurs the boundaries will lose some particles and acquire others, and therefore the overall particle coarsening rate may be uniform, although the rate constant in equation 11.37 should include a correction factor to account for the fraction of the time a particle is not attached to a boundary.

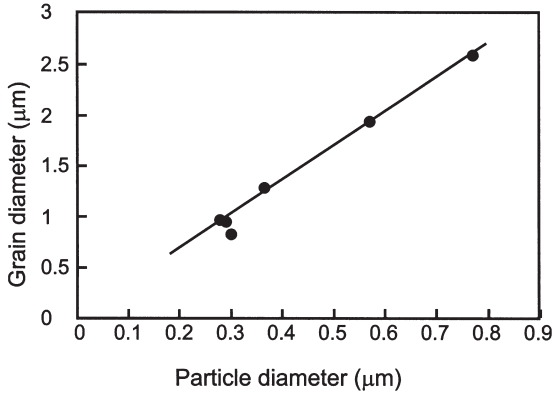

Fig. 11.14. The relationship between grain size and particle diameter for an Al–6wt%Ni alloy containing a volume fraction of 0.10 of $NiAl_3$ particles, (Humphreys and Chan 1996).

11.4.3.3 Coarsening of duplex microstructures

In a duplex alloy in which the volume fractions of the two phases are comparable, the rate of coarsening of the structure is controlled by interdiffusion between the phases over distances which are of the order of the size of the phases. In this situation the coarsening rate is predicted to be dependent on the coarsening mechanism and morphology and volume fractions of the phases (e.g. Ardell 1972, Martin and Doherty 1976). A detailed analysis of such phase growth is beyond the scope of this book, but typically, it is expected that the growth exponent will be ~3 for bulk diffusion control (equation 11.37) and ~4 for interface control (equation 11.38). Grewel and Ankem (1989, 1990) have studied grain growth in a variety of titanium-based alloys containing a wide range of volume fractions, such as the microstructure shown in figure 11.15 and find that, as shown in figure 11.16, the growth exponent is not particularly sensitive to volume fraction. However, it is found that as the temperature is raised from 700°C to 835°C the growth exponent **n** in Ti–Mn alloys decreases from 3.6 to 3.1, indicating a change in growth mechanism from interface to bulk diffusion control with increasing temperature.

Although Higgins et al. (1992) reported a growth exponent of ~4 for duplex Ni–Ag alloys, which is consistent with interface diffusion-controlled coarsening as discussed above, they found that the rate constants were several orders of magnitude greater than predicted by the theory of Ostwald ripening. They suggested that the non-spherical shape of the particles (e.g. fig. 11.15) and the resulting curvature provide a driving force for **particle migration and coalescence**.

11.4.4 Grain rotation

Randle and Ralph (1987) found that in a nickel-based superalloy in which grain growth was inhibited by the second-phase particles, there was a much higher frequency (~50%)

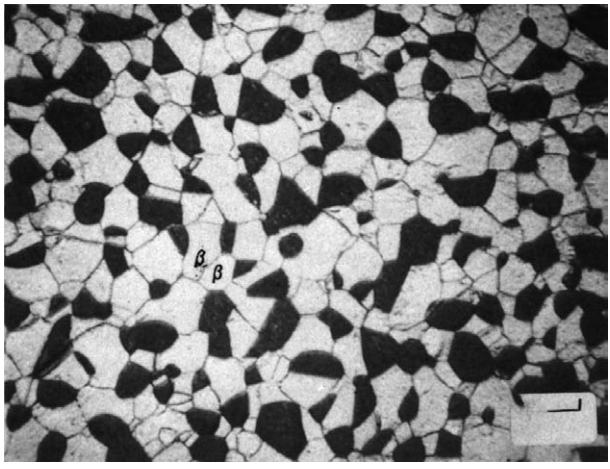

Fig. 11.15. Microstructure of a Ti–6%Mn alloy containing 44% of α-phase (dark) and 56% of β-phase, (Grewel and Ankem 1990).

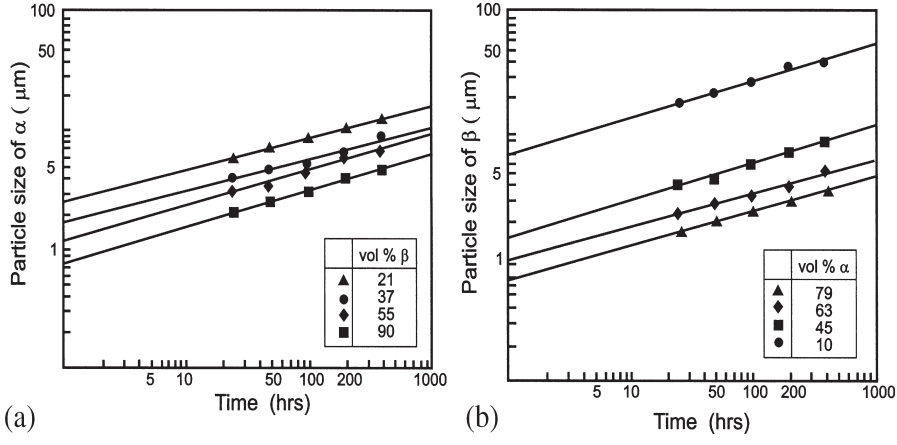

Fig. 11.16. Growth kinetics of the phases in a series of Ti–Mn alloys containing different volume fractions at 973K, (a) α-phase, (b) β-phase, (Grewel and Ankem 1989).

of low-Σ boundaries than in the same alloy in which precipitation had not occurred. It was suggested that this might be the result of grains rotating to produce lower energy boundaries (cf. subgrain rotation in §6.5.4), although there is as yet no direct experimental evidence to support this proposed mechanism, and as discussed in §11.3.2, a high frequency of special boundaries may often arise as a result of grain growth by boundary migration, or during the recrystallization of particle-containing alloys (§7.7.4.3). However, 2-D molecular dynamics simulations (§6.5.4.5 and fig. 6.27) have suggested that nanoscale grains may rotate at temperatures close to the melting temperatures.

11.4.5 Dragging of particles by boundaries

Equation 11.26 shows that grain growth in a particle-containing material occurs when the driving pressure (P) is greater than the pinning pressure (P_z), and in the subsequent discussions it has been assumed that growth ceases at a limiting grain size when these two pressures are equal. However, the pressure exerted by a boundary on a particle may, at high temperatures, be sufficient to drag the particle through the matrix, and in these circumstances boundary migration will continue at a rate determined by the mobility of the particle in the matrix (M_p) (Ashby 1980, Gottstein and Schwindlerman 1993).

The effect of driving pressure on boundary velocity is shown schematically in figure 11.17. For low driving pressures, ($P < P_z$) the boundary moves together with the particles and the velocity is given by

$$v = \frac{M_P P}{N_s} \tag{11.39}$$

where N_s is the number of particles per unit area of boundary.

However, when $P > P_z$ the boundary breaks away from the particles and velocity is given by $M(P - P_z)$, where M is the intrinsic mobility of the boundary (i.e. equation 11.26).

There are several mechanisms by which the particles can move through the matrix (Ashby 1980), including the migration of atoms (matrix or particle) by diffusion through the matrix, through the particle or along the interface. Ashby (1980) has shown that in general, coupled diffusion of both matrix and particle atoms is required. The resulting particle mobilities are low and are generally negligible for stable crystalline particles. However, for gas bubbles or amorphous or liquid particles, measurable particle velocities may occur at very high temperatures (Ashby 1980).

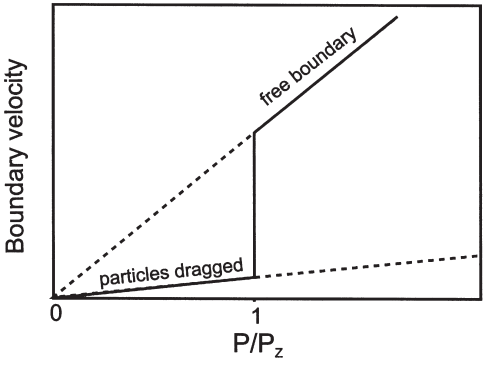

Fig. 11.17. The grain boundary velocity as a function of the driving pressure (P). At low driving pressures the boundary velocity is controlled by the dragging of particles, but when the driving pressure exceeds the pinning pressure due to particles (P_z), the boundary breaks free from the particles.

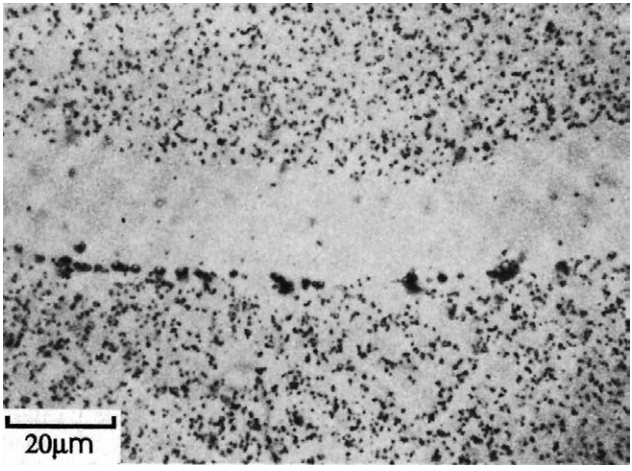

Fig. 11.18. Particle dragging by a boundary in copper containing amorphous SiO_2 particles. The particle-free band behind the migrating boundary and the increased particle concentration at the boundary are clearly seen, (Ashby and Palmer 1967).

Ashby and Centamore (1968) observed particle drag in copper containing various oxide dispersions annealed at high temperatures. As particles are swept along with the boundary, the number of particles on the boundary (N_s) increases as is seen in figure 11.18, and therefore the boundary velocity decreases according to equation 11.39. The mobilities of amorphous SiO_2, GeO_2 and B_2O_3 particles were all measurable at high temperatures, but significantly no migration of stable, crystalline Al_2O_3 particles was detectable. This phenomenon is therefore unlikely to be important in alloys containing stable crystalline particles. However, if such a mechanism were to occur in an engineering alloy, the resulting increased concentration of particles at grain boundaries would be expected to lead to increased brittleness and susceptibility to corrosion.

11.5 ABNORMAL GRAIN GROWTH

In the previous section we discussed the uniform growth of grains following recrystallization. There are however, circumstances when the microstructure becomes unstable and a few grains may grow excessively, consuming the smaller recrystallized grains (fig. 11.1b). This process, which may lead to grain diameters of several millimetres or greater is known as **abnormal grain growth.** Because this **discontinuous growth of selected grains** has similar kinetics to primary recrystallization and has some microstructural similarities, as shown in figure 11.19, it is sometimes known as **secondary recrystallization.** Abnormal grain growth is an important method of producing large grained materials and contributes to the processing of Fe–Si alloys for electrical applications (§15.4). The avoidance of abnormal grain growth at high temperatures is an important aspect of grain size control in steels and other alloys, and Dunn and Walter (1966) give an extensive review of abnormal grain growth in a wide variety of materials.

Fig. 11.19. Abnormal grain growth in Al–1%Mg–1%Mn annealed at 600°C.

11.5.1 The phenomenon

The driving force for abnormal grain growth is usually the reduction in grain boundary energy as for normal grain growth. However, in thin materials an additional driving force may arise from the orientation dependence of the surface energy (§11.5.4). Abnormal grain growth originates by the preferential growth of a few grains which have some special growth advantage over their neighbours, and the progress of abnormal grain growth may be described in some cases by the JMAK kinetics of equation 7.17 (Dunn and Walter 1966).

An important question to consider is whether or not abnormal grain growth can occur in an 'ideal grain assembly' i.e. one in which there are no impurities and the boundary energy is constant. As was shown by Thompson et al. (1987), the answer to this question can be deduced from the theory of grain growth, and we will base our discussion on the analysis presented in chapter 10.

Consider the growth of a particular grain of radius R in an assembly of grains of mean radius $\bar{R}$. The growth rates of the grain and the assembly are given by equations 10.10. and 10.13 respectively, and the condition for the abnormal growth of the particular grain is given by equation 10.14. For the 'ideal' material, all boundary energies and mobilities are equal and the condition for abnormal growth then becomes

$$\frac{4R}{R} - \frac{R^2}{R^2} - 4 > 0 \tag{11.40}$$

This condition is never achieved, although the left hand side equals zero when $R = 2\bar{R}$.

Thus a very large grain will always grow more slowly than the average grain relative to the grain assembly, and will eventually rejoin the normal size distribution. Therefore abnormal grain growth cannot occur in an 'ideal grain assembly'.

Monte-Carlo simulation of abnormal grain growth (Srolovitz et al. 1985) has been found to produce a similar result. Abnormal grain growth can therefore only occur

when normal grain growth is inhibited, unless the abnormally growing grain enjoys some advantage other than size over its neighbours. The main factors which lead to abnormal grain growth – **second-phase particles**, **texture** and **surface effects**, are considered below.

11.5.2 The effect of particles

As discussed in §11.4.2, a dispersion of second-phase particles will prevent growth above the limiting grain size. However, under certain circumstances, abnormal grain growth may still be possible. This phenomenon has been analysed by many people, the best known work being that of Hillert (1965) and Gladman (1966). In the following section, we explore, using the cellular stability model of chapter 10, the conditions under which abnormal grain growth occurs, and will reach conclusions which are in general agreement with the earlier work.

11.5.2.1 Conditions for abnormal grain growth

As discussed in §11.5.1, abnormal grain growth is an example of unstable or discontinuous growth of a cellular microstructure, and may be analysed accordingly. We will assume for the moment that all the grain boundary energies and mobilities are equal, and that the material, containing grains of mean radius $\bar{\mathbf{R}}$, and a volume fraction $\mathbf{F_V}$ of spherical particles of diameter **d.**

From equation 10.22 we see that $d\bar{R}/dt$ will become zero and thus normal grain growth will cease when

$$\Psi = \frac{1}{4} \tag{11.41}$$

where $\Psi = 3F_V\bar{R}/d$ (equation 10.21), and therefore the limiting grain size is

$$\bar{R}_{LIM} = \frac{d}{12\,F_V} \tag{11.42}$$

The limiting grain size, $\bar{R}_{LIM}$ as given by equation 11.42 is seen to be identical to the limiting grain size (D_Z) of equation 11.30, with the constant $\alpha = 0.25$, which is within the limits consistent with experimental observations (§11.4.2.1).

For $\Psi > 0.25$, it may be seen from inequality 10.12 that because $d\bar{R}/dt$ is always zero, abnormal grain growth will always occur provided that dR/dt is positive. As shown in figure 11.20, the **minimum** size of grain to initiate abnormal growth is small for $\Psi < 0.5$. However, the **maximum** size ratio which can be achieved by abnormal growth is less than 5 if $\Psi < 0.1$ (or $F_V/d < 1/30\bar{R}$). Below this value of Ψ we therefore find a **broadening of the grain size distribution rather than true abnormal growth.** As Ψ increases above 0.25, the minimum size of grain required to initiate abnormal growth increases, and it is seen from equation 10.23 that growth becomes impossible for even the largest abnormally growing grain if $\Psi \geq 1$ or

$$\frac{F_V}{d} > \frac{1}{3\bar{R}} \tag{11.43}$$

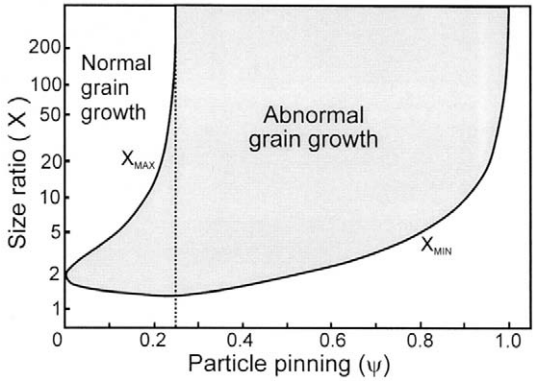

Fig. 11.20. The effect of particles (expressed in terms of the dimensionless parameter Ψ) on the minimum grain size ratio (X_{MIN}) required to initiate abnormal grain growth in an ideal grain assembly, and the maximum ratio (X_{MAX}) to which such grains may eventually grow. Note that for small values of Ψ, X_{MAX} is sufficiently small that size broadening rather than discontinuous grain growth will occur, (Humphreys 1997b).

which corresponds to a mean grain size (D_M) of

$$D_M = 2\mathbf{R} = \frac{2d}{3F_V} \tag{11.44}$$

and therefore above this dispersion level no grain growth of any type can occur. D_M is seen to be four times the limiting grain size for normal grain growth given by equation 11.42. These predictions (and figure 11.20) are similar to the conclusions reached in the much more detailed model of Anderson et al. (1995). From our model we can identify 5 distinct regimes:

$\Psi = 0$	**Normal grain growth possible**
$0 < \Psi < 0.1$	**Broadening of grain size distribution**
$0.1 < \Psi < 0.25$	**Abnormal growth and normal grain growth**
$0.25 < \Psi < 1$	**Abnormal growth but no normal grain growth**
$\Psi > 1$	**No growth possible**

These regimes are shown in figure 11.21 as a function of the mean grain size ($\bar{\mathbf{R}}$) and the dispersion level (F_V/d). The upper limit of Ψ for abnormal growth shown in figure 11.21 is the condition for migration of a planar boundary ($R = \infty$) and this assumes that abnormal grain growth is not limited by the availability of a suitably large grain as a 'nucleus'. However, as seen from figure 11.20, at larger values of Ψ the minimum grain size required to initiate abnormal grain growth increases and the largest available grain will depend on the size distribution in the grain assembly. It is often found that grain size distributions are log-normal and that the maximum is typically $\sim 2.5\bar{\mathbf{R}}$ (e.g. fig.11.6). From equation 10.25, it can be shown that this corresponds to $\Psi \sim 0.6$ and this condition, which is a more realistic limit to abnormal grain growth is shown as a dotted line in figure 11.21. It should be noted that this analysis is based on the pinning due to

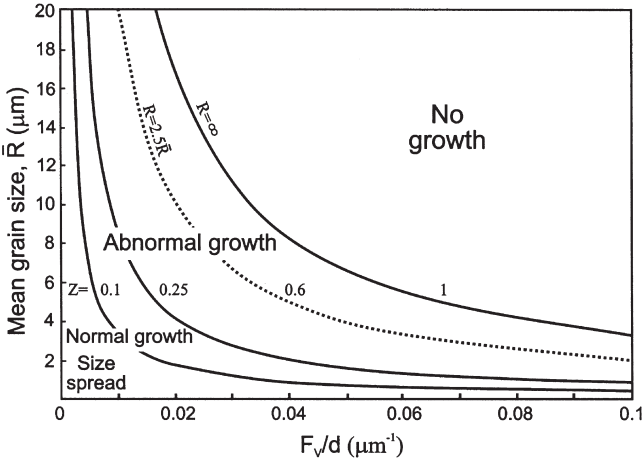

Fig. 11.21. The various growth regimes for an ideal grain assembly as a function of the matrix grain size ($\bar{R}$) and the particle dispersion level (F_V/d). The dotted line corresponds to $\Psi = 0.6$, which is the condition for the abnormal growth of a grain of diameter 2.5 times that of the assembly, (Humphreys 1997b).

particles being the Zener pinning pressure (equation 4.24), and as discussed in §4.6.2.2 and §11.4.2.3, this may not be appropriate for large particle volume fractions.

Alloys which have been processed to produce grain sizes of less than a micrometre are currently of considerable scientific and technological interest (§15.6), and the conditions for abnormal grain growth in these materials are further discussed in §14.5.2.

11.5.2.2 Experimental observations

Abnormal grain growth has been reported for a large number of alloys containing particle volume fractions of between 0.01 and 0.1, and details may be found in Dunn and Walter (1966), Cotterill and Mould (1976) and Detert (1978). However, there is very little evidence in the literature as to the precise conditions necessary to induce or prevent this phenomenon. The fact that abnormal grain growth does not occur more readily in particle-containing alloys may be due to a number of factors.

(i) In many cases the grain size produced during primary recrystallization is significantly greater than the particle-limited grain size, and Hillert (1965) noted that this is a very effective way of suppressing abnormal grain growth. According to the analysis above, abnormal grain growth will not be possible if the grain size is larger than four times the limiting grain size for normal grain growth. As discussed in §9.2.1, the grain size produced by primary recrystallization is a complex function of the particle parameters and the thermomechanical processing route, and in alloys in which the ratio F_V/r is large, particle pinning often results in a large grain size after primary recrystallization. As an example, consider the recrystallization data shown in figures 9.2 and 9.3 for particle-containing

aluminium alloys which exhibit accelerated and retarded recrystallization. Data for two specimens from each investigation (the extreme data points of each figure), are summarized in table 11.3. It can be seen that particularly for the material showing retarded recrystallization (material code1), the measured grain size is very much larger than the limiting grain size (D_Z) as given by equation 11.42, (or equation 11.30 with $\alpha = 0.25$). If the measured grain sizes are compared with D_M, the critical grain size for abnormal grain growth (equation 11.44), it may be seen that abnormal grain growth will not be possible in materials 1 or 2, but is highly likely in materials 3 and 4.

(ii) The occurrence of abnormal grain growth may be limited by 'nucleation' rather than growth considerations. Strong evidence for this comes from the large number of experimental observations which show that abnormal grain growth is particularly likely to occur as the annealing temperature is raised and as the particle dispersion becomes unstable. This is clearly shown in the classic early work of May and Turnbull (1958) on the effect of MnS particles on abnormal grain growth in silicon iron. Gladman (1966, 1992) has discussed the unpinning of boundaries under conditions of particle coarsening, with particular reference to steels in which the control of abnormal grain growth is of great technological importance, and the grain growth behaviour of some steels is shown in figure 11.22.

Plain carbon steels without grain refining additives show a coarsening of the grain size by normal grain growth. However, if conventional grain growth inhibitors (AlN) are present (fig. 11.22a), then small grains persist up to a temperature of ~1050°C at which temperature coarsening of the particles allows abnormal grain growth to occur, producing a very large grain size. At temperatures of ~1200°C, most of the particles have dissolved and normal grain growth then results. However, if a coarser dispersion

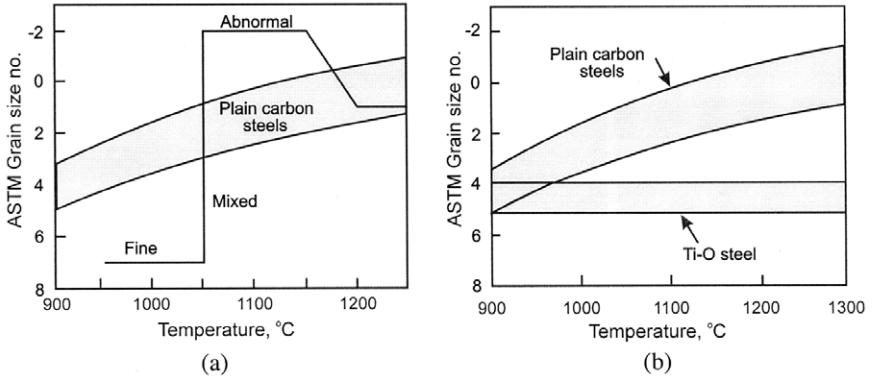

Fig. 11.22. Abnormal grain growth in steels. (a) TiN grain growth inhibitors are very effective in preventing normal grain growth, but their coarsening and dissolution lead to abnormal grain growth at high temperatures, (b) Coarse, insoluble, non-metallic inclusions are less effective in preventing normal grain growth, but their stability prevents abnormal grain growth, (Gladman 1992).

Table 11.3
Conditions for abnormal grain growth in some particle-containing aluminium alloys.

Code	Alloy	F_V	d (μm)	Grain Size (μm)	D_M (μm)	D_Z (μm)	Reference
1	Al–Cu	0.053	0.56	1483	11	2.5	Doherty and Martin (1964)
2	Al–Cu	0.03	1.01	68	67	15.7	
3	Al–Si	0.0012	0.7	160	583	114	Humphreys (1977)
4	Al–Si	0.01	4.9	44	490	16.3	

of more stable particles (e.g. oxides or titanium carbonitrides) is present (fig. 11.22b) then all grain growth is inhibited to very high temperatures.

According to the analysis of §11.5.2.1 as summarised in figure 11.21, if an alloy which is stable against abnormal growth is annealed at a temperature where the particles coarsen or the volume fraction decreases (i.e. lower F_V/d), abnormal grain growth will only become possible if the mean grain size does not increase proportionately. The onset of abnormal grain growth may then depend on local destabilization of the grain structure by removal or weakening of critical pinning points (Gladman 1966), leading to local inhomogeneous grain growth. The resulting broader grain size distribution may then enable the 'nucleation' of abnormal grain growth.

11.5.2.3 Computer simulation

Monte-Carlo simulations of abnormal grain growth in the presence of particles have been carried out in 2-D (Srolovitz et al. 1985) and 3-D (Doherty et al. 1990). In 2-D, although normal grain growth stagnated due to particle pinning, abnormal grain growth could not be induced. However, in the 3-D simulations, large artificially-induced grains were found to be stable and to consume the smaller pinned grains, which is in keeping with the analytical models discussed above and with the experimental observations. This result again emphasises the necessity of using 3-D simulations for the modelling of particle pinning.

11.5.3 The effect of texture

The inhibition of normal grain growth by texture (§11.3) may lead to the promotion of abnormal grain growth, and a review of the extensive work in this field is given by Dunn and Walter (1966) and Cotterill and Mould (1976). Perhaps the best example of this is the intensification of the Goss texture in silicon iron, which is discussed in (§15.4). In many cases normal grain growth is restricted by a number of factors such as particles and free surfaces in addition to texture, in which case it is difficult to quantify the role of texture in abnormal grain growth.

If a **single strong texture component** is present in a fine-grained recrystallized material, then abnormal grain growth commonly occurs on further annealing at high

temperatures. This has been clearly demonstrated for the cube texture in aluminium (Beck and Hu 1952), copper (Dahl and Pawlek 1936, Bowles and Boas 1948, Kronberg and Wilson 1949), nickel alloys (Burgers and Snoek 1935) and silicon iron (Dunn and Koh 1956).

Abnormal grain growth is possible in such a situation because within a highly textured volume the grain boundaries have a lower misorientation and hence a lower energy and mobility than within a normal grain structure. If some grains of another texture component are present, then these introduce boundaries of higher energy and mobility which may migrate preferentially by a process which is therefore closely related to primary recrystallization of a material containing subgrains (chapter 7).

Analyses of abnormal grain growth in a textured material have been carried out by e.g. Abbruzzeze and Lücke (1986) and Eichelkraut et al. (1988). The analysis discussed below is based on the model of Humphreys (1997a), which is presented in chapter 10. A somewhat similar analysis which considered only the effects of boundary mobility and not boundary energy, was given by Rollett et al. (1989b).

Abnormal grain growth tends to occur when there is at least one strong texture component. If this texture component is very sharp, then the mean misorientation ($\bar{\theta}$) is small and there are many low angle boundaries within a particular texture variant, whereas if the texture component is more diffuse then the boundaries have a higher mean misorientation. Typically, a texture component is defined as containing orientations within $\sim 15^\circ$ of some ideal orientation and therefore we could take $\bar{\theta} = 15^\circ$ as an upper limit for the grain/subgrain assembly in our model. There will be other grains in the microstructure which have either 'random' orientation, are part of another texture component or are a crystallographic variant of the main component. Thus we expect the microstructure to contain many high angle boundaries ($\bar{\theta} > 15^\circ$) and these will provide the 'nuclei' for discontinuous growth. The situation will therefore be similar to that shown in fig.10.3b for $\bar{\theta}$ in the range 5° to 15°, where we note that nucleation of abnormal grain growth will be easy, but the maximum size ratio of the abnormally growing grains will be small if the main texture component is diffuse (large $\bar{\theta}$). For example figure 10.3b indicates that if $\theta = 10^\circ$, the maximum size of abnormally growing grains will be approximately five times the mean grain size.

Diffuse textures: Hutchinson and Nes (1992) noted that in steel, Cu and Al, grains in the main texture components were larger than average, and similar results were reported during grain growth of Al–Mn (Distl et al. 1982, Weiland et al. 1988). These results may be demonstrating the transitional normal/abnormal behaviour predicted for grain assemblies with medium angle boundaries discussed above, for which broad size distributions rather than true abnormal growth, are predicted.

Strong textures: If the main texture component is strong, then $\bar{\theta}$ is small and stronger abnormal growth is predicted (fig.10.3a). This is amply confirmed by experiment, a good example being silicon iron (§15.4). The model presented in chapter 10, predicts that the maximum size ratio of the abnormal grains to the grain assembly should decrease as the main texture component is weakened, and quantifies the relationship between these parameters. Although this is broadly in line with experiments, there are few measurements quantitatively relating texture strength and grain size distribution.

11.5.4 Surface effects

It has long been recognised that abnormal grain growth is often easier in thin sheets than in bulk materials. This phenomenon is of particular importance in the production of sheet Fe–Si alloys (Dunn and Walter 1966) as is discussed in §15.4. The control of grain size and texture in the thin polycrystalline films used for electronic applications provides a more recent example of the importance of surface effects in grain growth (Abbruzzese and Brozzo 1992, Thompson 1992). Abnormal grain growth may occur in thin sheets if normal grain growth is inhibited by the free surfaces or by particles or texture as discussed above, and is particularly favoured if the texture leads to a significant variation of surface energy among the grains, as illustrated by the recent work of Greiser et al. (2001).

11.5.4.4 Surface inhibition of normal grain growth

When grains are of the order of the thickness of the sheet, then the grains are significantly curved only in one direction, and from equation 11.1, the driving pressure is seen to fall towards half that of a grain within a 3-D assembly. Thermal grooving at the junction between the boundary and the free surface, due to the balance between the surface tension and grain boundary tension may also exert a pinning effect on the boundary. The classic work on thermal grooving is due to Mullins (1958) and this treatment has been extended by Dunn (1966), Frost et al. (1990) and Frost et al. (1992). An application of Frost's computer model to the simulation of grain growth in thin metallic strips is shown in figure 16.9.

The following is a simplified treatment of the phenomenon.

Consider a single grain in a sheet of thickness **S,** whose boundaries are pinned by thermal grooving as shown in figure 11.23. The angle θ_g at the thermal groove as shown in figure 11.23b is determined by the balance between the forces arising from the boundary energy γ_b and the surface energy γ_{sur} and is given by

$$\theta_g = \arcsin\left(\frac{\gamma_b}{2\gamma_{sur}}\right) = \frac{\gamma_b}{2\gamma_{sur}} \tag{11.45}$$

The boundary can be pulled out of the groove if, at the surface, it deviates from the perpendicular by an angle of $\sim\theta_g$, which corresponds to a radius of curvature of

$$R_2 = \frac{S}{2\theta_g} \tag{11.46}$$

which can be equated with a pinning pressure due to thermal grooving of

$$P_g = \frac{\gamma_b^2}{S\gamma_{sur}} \tag{11.47}$$

This is opposed by the pressure **P** (equation 11.3) due to the in-plane curvature $\mathbf{R_1}$, (fig.11.23a). Thus, no grain growth will occur if $P_g \geq P$, and therefore the limiting grain

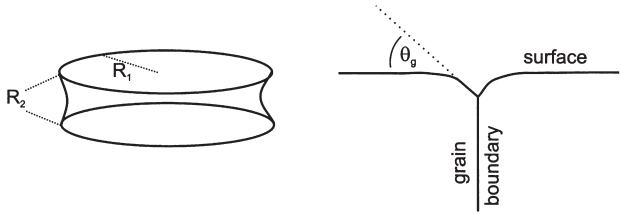

Fig. 11.23. Thermal grooving of a thin specimen. (a) The shape of an isolated grain in a thin sheet, (b) Thermal grooving at the surface.

size for normal grain growth (D_L) is given as

$$D_L = \frac{S c_1 \gamma_{sur}}{\gamma_b} \tag{11.48}$$

where c_1 is a small constant.

Mullins (1958) proposes that $c_1 = 0.8$, and computer simulations by Frost et al. (1992) give $c_1 \sim 0.9$. Typically, it is found that $\gamma_{sur} \sim 3\gamma_b$, suggesting a limiting size for normal grain growth in thin films of 2 to 3 times the thickness, which is consistent with experimental measurements in metals (Beck et al. 1949) and semiconductor films (Palmer et al. 1987).

11.5.4.5 Abnormal grain growth in thin films

There is considerable evidence that abnormal grain growth can readily occur in thin films or sheets in which normal grain growth has stagnated for the reasons discussed above (Beck et al. 1949, Dunn and Walter 1966, Palmer et al. 1987, Thompson 1992). That this abnormal grain growth is **not driven by boundary curvature** is clear from observations which show that the direction of motion may be in the opposite direction to that predicted by the curvature (Walter and Dunn 1960b), and from measurements which show that the boundary velocity is constant with time (Rosi et al. 1952, Walter 1965). Two dimensional computer simulations of grain growth are particularly effective for studying abnormal grain growth in thin films (Srolovitz et al. 1985, Rollett et al. 1989b, Frost and Thompson 1988).

The driving pressure for abnormal grain growth comes from the orientation dependence of the surface energy. If the difference in surface energy between two adjacent grains is $\Delta\gamma_{sur}$ then the driving pressure for boundary migration is $P_s = 2\Delta\gamma_{sur}/S$. As this has to overcome the drag due to thermal grooving the growth velocity will be

$$v = M(P_s - P_g) = \frac{M}{S}\left(2\Delta\gamma_{sur} - \frac{\gamma_b^2}{\gamma_{sur}}\right) \tag{11.49}$$

The velocity of abnormal grain growth is thus predicted to be inversely proportional to the sheet thickness, which is consistent with experiments on metal sheet (Foster et al. 1963) and semiconductor thin films (Palmer et al. 1987).

The condition that abnormal grain growth should occur is given from equation 11.49 as

$$2\Delta\gamma_{sur} > \frac{\gamma_b^2}{\gamma_{sur}} \tag{11.50}$$

or

$$\frac{\Delta\gamma_{sur}}{\gamma_{sur}} > c_2\left(\frac{\gamma_b}{\gamma_{sur}}\right)^2 \tag{11.51}$$

where c_2 is a small constant which is given by Mullins (1958) as 1/6 and Frost et al. (1992) as $\sim$1/4.

Taking $\gamma_{sur}/\gamma_b = 3$, then equation 11.51 indicates that abnormal grain growth will occur if $\Delta\gamma_{sur} > 0.02\gamma_{sur}$, i.e. only a few percent difference in surface energy is required to promote abnormal grain growth in thin specimens.

Surface energy variations between grains are a consequence of grain orientation. Therefore the analysis above, which takes account of the variation of **surface energy** due to orientation but not the variation of the **grain boundary energy** due to texture, must be an oversimplification.

The surface energy of a grain is of course very dependent on the surface chemistry, and it has long been known that abnormal grain growth in Fe–Si alloys is affected by the atmosphere (Detert 1959, Walter and Dunn 1959, Dunn and Walter 1966). Recent work on grain oriented, silicon steel sheet (§15.4) has shown the importance of small alloying additions in determining surface energies.

11.5.5 The effect of prior deformation

There has been interest in the effects of small strains on grain growth and abnormal grain growth (Riontino et al. 1979, Randle and Brown 1989). The observation that a small prior plastic strain may prevent normal grain growth and promote the onset of anomalous grain growth has long been known (§1.2.1.3) and is probably best interpreted in terms of **primary recrystallization by strain induced boundary migration** (§7.6.2) rather than as a grain growth phenomenon.